POLYPUBLIE
Polytechnique Montréal

POLYTECHNIQUE
MONTRÉAL

UNIVERSITÉ
D'INGÉNIERIE

Titre: Title:	Modeling and Aggregation of Thermostatically Controlled Loads for Participation in Frequency and Voltage Control of a Power System
Auteur: Author:	Imen Jendoubi
Date:	2019
Type:	Mémoire ou thèse / Dissertation or Thesis
Référence: Citation:	Jendoubi, I. (2019). Modeling and Aggregation of Thermostatically Controlled Loads for Participation in Frequency and Voltage Control of a Power System [Mémoire de maîtrise, Polytechnique Montréal]. PolyPublie. https://publications.polymtl.ca/3974/

Document en libre accès dans PolyPublie
Open Access document in PolyPublie

URL de PolyPublie: PolyPublie URL:	https://publications.polymtl.ca/3974/
Directeurs de recherche: Advisors:	Keyhan Sheshyekani, & Houshang Karimi
Programme: Program:	Génie énergétique

POLYTECHNIQUE MONTRÉAL

affiliée à l'Université de Montréal

Modeling and aggregation of thermostatically controlled loads for participation in frequency and voltage control of a power system

IMEN JENDOUBI

Département de génie électrique

Mémoire présenté en vue de l'obtention du diplôme de *Maîtrise ès sciences appliquées*
Génie énergétique

Août 2019

POLYTECHNIQUE MONTRÉAL

affiliée à l'Université de Montréal

Ce mémoire intitulé :

Modeling and aggregation of thermostatically controlled loads for participation in frequency and voltage control of a power system

présenté par **Imen JENDOUBI**
en vue de l'obtention du diplôme de *Maîtrise ès sciences appliquées*
a été dûment accepté par le jury d'examen constitué de :

Jean MAHSEREDJIAN, président
Keyhan SHESHYEKANI, membre et directeur de recherche
Houshang KARIMI, membre et codirecteur de recherche
Hanane DAGDOUGUI, membre

ACKNOWLEDGEMENTS

RÉSUMÉ

L'opération d'un réseau électrique est un acte de balancement puisque l'équilibre entre la production et la consommation doit être maintenue en temps réel. La fréquence et la tension sont des indicateurs précis des déséquilibres et doivent par conséquent être maintenues dans les limites autorisées pour un fonctionnement stable des réseaux électriques. Traditionnellement, l'équilibre entre la production et la consommation est assuré par les générateurs conventionnels fonctionnant aux combustibles fossiles. Or, ce moyen est économiquement inefficace et a un impact négatif sur l'environnement. La pénétration croissante des sources d'énergie renouvelable complique plus que jamais l'équilibre production-consommation puisqu'elles induisent davantage des fluctuations, ce qui accroît le besoin en réserves de contrôle à réaction rapide. La réponse à la demande est une des solutions efficaces, économiques et à impact environnemental positif pouvant prendre part dans la provision des réserves de contrôle, surtout avec le développement des technologies et techniques des réseaux intelligents. En particulier, les charges thermiquement contrôlées (TCLs) sont des candidats potentiels car elles sont nombreuses et largement distribuées dans le réseau électrique. De plus, les TCLs sont des appareils à action rapide et peuvent être gérées sans compromettre le confort du client.

L'objectif principal de ce travail est l'implication des TCLs dans la provision du contrôle primaire et secondaire de la fréquence ainsi que la régulation de la tension. Par conséquent, un défi important consiste à développer une stratégie de contrôle fiable et à réaction rapide pour une participation efficace des TCLs dans de tels services auxiliaires. De plus, cela devrait être fait en tenant compte du confort du client, de l'usure des appareils et des problèmes liés aux cycles courts. De plus, une estimation et prévision précises des réserves de contrôle disponibles offertes par les TCLs sont essentielles. A cette fin, une approche basée sur un réseau de neurones est proposée pour l'estimation et la prévision précises de la flexibilité disponible offerte par les TCLs. Une comparaison entre cette nouvelle approche et l'approche conventionnelle basée sur la chaîne de Markov montre une précision de prédiction supérieure de l'approche basée sur un réseau de neurones. Des méthodes de contrôle sont ensuite développées pour une gestion efficace et optimale d'une population de TCLs via un agrégateur afin d'obtenir une réponse collective imitant le comportement des générateurs conventionnels, tout en respectant les exigences des services de contrôle fournis. En particulier, la participation des TCLs au contrôle primaire de la fréquence est semi-autonome et ne repose pas sur une communication en temps réel bénéficiant de la réponse rapide des TCLs. Les méthodes de contrôle proposées se caractérisent par une réponse rapide et un très faible

fardeau de communication, tout en maintenant le confort du client, en minimisant le nombre de commutions ON/OFF grâce à une priorisation appropriée des TCLs et en réduisant le phénomène des cycles courts par la division des TCLs en groupes.

Les méthodes de contrôle proposées pour gérer des agrégations de TCLs en tant que générateurs virtuels sont incorporées dans un système de gestion de l'énergie (EMS) hiérarchisé pour permettre la coordination entre les TCLs et d'autres ressources conventionnelles du réseau afin de fournir un contrôle primaire/secondaire de fréquence et de tension dans un micro-réseau. Seuls les TCLs ayant une consommation d'énergie active et réactive peuvent participer au contrôle secondaire, de sorte qu'ils puissent affecter les flux de puissance actives et réactives. En particulier, le contrôle secondaire est formulé sous la forme d'un problème d'optimisation multi-objectifs basé sur un calcul de flux de puissance (PF) afin de minimiser simultanément les écarts de fréquence/tension et le coût d'opération du réseau. La méthode de la région de confiance est adoptée pour résoudre les équations de PF de manière fiable. Une série de simulations réalisée pour un micro-réseau moyenne tension montre l'efficacité de la participation des TCLs à la régulation de fréquence et de tension d'un réseau.

ABSTRACT

Operating an electric power system is a balancing act as the equilibrium between generation and consumption must be maintained in real-time. Frequency and voltage are accurate indicators of imbalances, and therefore must be kept within permissible ranges for a stable operation of power systems. Traditionally, the generation-consumption balancing is provided by fossil-fueled conventional generators which are economically inefficient and environmentally unfriendly. The increasing penetration of renewable energy sources is making the balancing more challenging than ever as they induce further fluctuations, which in turn increase the need for fast-responding control reserves. Demand Response is one of the efficient, cost-effective and environment-friendly alternatives for taking part in the provision of control reserves, especially with the development of smart grid technologies and techniques. In particular, thermostatically controlled loads (TCLs) are potential candidates as they are numerous and widely distributed in the electrical network. Furthermore, TCLs are fast-acting devices and can be managed without compromising customer comfort.

The main objective of this work is the implication of TCLs in the provision of primary and secondary frequency control as well as voltage regulation. In this way, an important challenge is to develop a reliable and fast reacting control strategy for an efficient participation of TCLs in such ancillary services. Furthermore, this should be done taking into account customer comfort, device wear and tear, and short cycling issues. Moreover, an accurate estimation and prediction of the available control reserves offered by TCLs are essential. To this aim, a neural network-based approach is proposed for the accurate estimation and prediction of the available flexibility offered by TCLs. A comparison between this new approach and the conventional Markov-Chain approach shows a superior prediction accuracy of the neural network-based approach. Control methods are then developed for an effective and optimal management of a population of TCLs through an aggregator in order to obtain a collective response that imitates the behaviour of conventional generators, while respecting the requirements of the provided control services. In particular, TCLs participation in primary frequency control is semi-autonomous with no reliance on real-time communication benefiting from TCLs fast response. The proposed control methods are characterized by a fast response and a very low communication burden, while the customer comfort is maintained, the switching number is minimized by proper prioritization of TCLs, and short-cycling is reduced by the division of TCLs into groups.

The proposed control methods for managing aggregations of TCLs as virtual generators

are incorporated within a hierarchical control-based Energy Management System (EMS) to enable the coordination among TCLs and other conventional grid resources for the provision of primary/secondary frequency and voltage control in a microgrid. Only TCLs that have active and reactive power consumption can participate in the secondary control so that they can affect both active and reactive power flows. In particular, the secondary control is formulated as a Power Flow (PF)-based multi-objective optimization problem in order to simultaneously minimize frequency/voltage deviations and grid operation cost. The Trust-Region method is adopted to reliably solve the PF equations. A set of simulations is carried out for a typical MV microgrid which shows the effectiveness of the participation of TCLs in the frequency and voltage regulation of a microgrid.

TABLE OF CONTENTS

LIST OF TABLES

LIST OF FIGURES

LIST OF SYMBOLS AND ACRONYMS

AQR   Automatic Q regulator

AVR   Automatic voltage regulator

CPP   Critical peak pricing

CV   Coefficient of variation

DER   Distributed energy resource

DG   Distributed generator

DLC   Direct load control

DR   Demand response

EI   Electronically-interfaced

EMS   Energy management system

ESS   Energy storage systems

FDI   Frequency deviation index

MO   Market operator

MOPSO   Multi-objective particle swarm optimization

PF   Power flow

RPC   Reactive power compensator

RTP   Real-time pricing

SG   Synchronous generator

TCL   Thermostatically controlled loads

TOU   Time-of-use

VDI   Voltage deviation index

CHAPTER 1   INTRODUCTION

1.1   Background and Motivation

The stable and reliable operation of power systems largely relies on maintaining real-time generation-consumption balance. The imbalances occasionally occur in the grid due to loss of a generator or a line, load changes, planning uncertainties, etc. Generally, these disturbances affect the frequency and/or voltage which are indicators of the imbalance between generation and demand, and therefore should be swiftly restored to their permissible ranges in order to maintain a stable and reliable power system operation [1]. The set of tools used by grid operators to accomplish this balance are referred to as 'ancillary services'. Generally, three control levels are applied to maintain the generation-consumption balance. The primary control has the fastest action (order of seconds) and aims to stabilize frequency and voltage and prevent further severe deviations. It is usually performed autonomously by generation units using local measurements and based on their droop characteristics. The secondary control aims to correct the voltage and frequency deviations still persisting after the action of the primary control and restore them to their nominal values. It has a slower response time (seconds to minutes) than primary control, hence it is usually implemented in a centralized manner. The tertiary control is manual and aims to restore primary and secondary control reserves usually through the re-dispatch of generation units. Traditionally, those services are prominently provided by fossil-fueled conventional generators [2–4].

Nowadays, due to the heading towards sustainable and green energy systems, the proliferation of renewable generation is a priority. For instance, Canada is one of the countries that has pledged to harness the renewable energy sources as an effective way to reach its ambitious goal of reducing greenhouse gas emissions by 30% until 2030 [5,6]. In the same vein, Denmark committed to phase-out all its fossil-fueled electricity in all sectors by 2050 [7]. A significant amount of the electrical energy from the renewable sources is provided by Wind Generation (WG) and Photovoltaic (PV) systems. These systems are characterized by an intermittent and stochastic behaviour in terms of energy generation. This makes generation-consumption balance more challenging than ever. To address this problem, one may think of whether quick-start units (i.e., conventional fossil-fueled generators) or (bulky) energy storage systems (ESS). Both solutions are, however, economically inefficient in particular for massive power generation. Moreover, the installation of fossil-fueled generators is vividly against the ultimate goal of reducing greenhouse gas emmissions [8]. Furthermore, as fluctuations might be successive and fast, addressing generators frequently causes mechanical harm and

increases the wear and tear [9]. Therefore, the reliance on traditional generators should be abridged by involving more efficient grid resources.

Adjusting the demand side rather than acting on the supply-side is an attractive solution which is the backbone of DR. Due to the development of smart metering, communication and control advancement, DR is expected to be a substantial and promising ingredient of the emerging smart grid paradigm [10]. According to the California Energy Commission, DR can be defined as "a reduction in customers' electricity consumption over a given time interval relative to what would otherwise occur in response to a price signal, other financial incentives, or a reliability signal" [11]. DR is capable of providing cost-effective and fast-response regulation resulting in enhanced overall system efficiency, while assisting the operation of the grid technically and economically [10]. In particular, Thermostatically controlled loads (TCLs) such as refrigerators, heat pumps, space heaters, air conditioners, and water heaters are considered potential DR resources. TCLs are electric devices that have the role of maintaining the temperature within a dead-band. TCLs are attractive DR resources for the participation in ancillary services since:

- TCLs are already existent in large numbers and therefore consume a large portion of the total electricity consumption. Considering the example of China, air conditioners are responsible for 30-40% of the peak power in summer [12]. In Canada, according to Natural Resources Canada, in 2016, heating represents around 61% of the total energy use of an average Canadian house as can be seen in Figure 1.1 [13].

- The number of TCLs is expected to grow significantly in the coming years. For example, according to the International Energy Agency, the stock of air conditioners is expected to grow from 1.6 billion in 2018 to 5.6 billion by 2050 [14]. It indicates that low initial investment is needed for the integration of TCLs in the provision of ancillary services unlike, for example, the expensive storage devices that require a considerable initial investment.

- TCLs operate within a temperature dead-band, hence they feature inherent flexibility to be managed without affecting customer comfort [15].

- TCLs are fast-responding devices, which makes them suitable for use in services that require a very fast response such as primary frequency control. As opposed to conventional generators with ramp-up and ramp-down rates, TCLs are characterized by a fast response as they promptly react to signals transmitted by the system operator with relatively no delay. The only delay related to the participation of TCLs is due to the communication link [15].

- Unlike conventional generators that require high costs even when used for short periods of time, TCLs have no cost when turned ON/OFF [15].

- Some TCLs are equipped with induction motors (e.g. heat pumps, refrigerators, HVACs, etc), which imply that they consume both active and reactive power. Such characteristics allow TCLs to have an impact on both active and reactive power flow in the grid, therefore on both frequency and voltage [16].
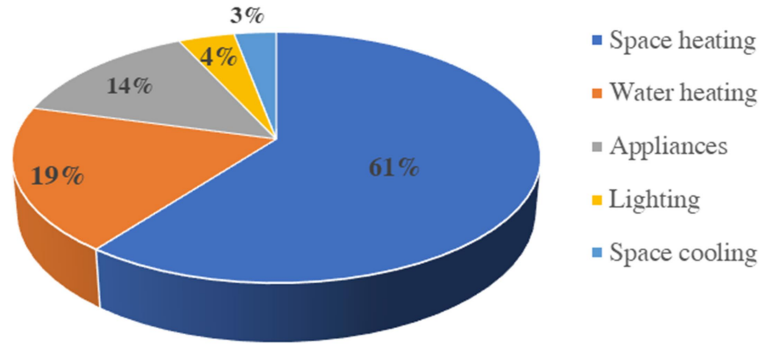
Figure 1.1 Residential energy consumption in a typical Canadian home in 2016 [13].

Despite the advantages mentioned above, in order to provide effective regulation services using TCLs, a key challenge is to develop a reliable and fast reacting control strategy for the provision of frequency and voltage control [17, 18]. A proper aggregation of TCLs is needed to obtain a collective behavior of TCLs that imitates the way conventional generators respond to deviations [17, 19]. In the meantime, customer comfort, device wear and tear, and short cycling issues should be taken into account. Furthermore, an aggregated model of a TCL population for the accurate estimation and prediction of the available control reserves (i.e. the aggregated power increase or decrease that can be offered by TCLs) is needed for effective exploitation and implication of TCLs in the energy market. As the focus of this work is on the implication of TCLs in the provision of frequency and voltage control in a power system, an appropriate aggregated model should take into account the dependency of the aggregated TCLs' response on various factors such as the ambient temperature, the frequency fluctuations, the voltage variations, etc.

There is a wide variety of works in the literature dealing with the incorporation of TCLs in the provision of primary and secondary frequency control. However, less attention has been given to TCLs' participation in voltage control mainly because TCLs are assumed purely resistive loads which is not always the case [16]. The integration of TCLs in the combined frequency and voltage control within the same control framework is of great interest as it limits the unfavorable effects resulting from the separate provision of each service, and leverages the full

potential of TCLs [20]. From one hand, It has been shown in various studies that correcting the frequency using controllable loads may result in under/over-voltages [21]. From the other hand, regulating the voltage at some nodes may result in unintentional over/under frequency [16]. However, only a few works have proposed control frameworks for simultaneous control of voltage and frequency [20, 22].

1.2 Research Objectives

The main objective of this work is to use TCLs in the provision of frequency and voltage control in a power system. To this aim, the research objectives are outlined as follows:

- Evaluating the effect of different external factors on the dynamic behavior of a TCL population.

- Developing a mathematical tool that accurately estimates and predicts the available control reserves that can be offered by a TCL population.

- Proposing control methods that allow managing a TCL cluster as a virtual generator for the provision of primary and secondary control.

- Incorporating the developed control methods into an EMS to enable optimal coordination of aggregations of TCLs with other conventional grid resources for the provision of control reserves.

1.3 Outline

- Chapter 2: This chapter provides first a background about DR, its programs, and benefits. Frequency and voltage control provision requirements within a power system are then presented. The third part introduces the TCLs aggregation concept. A review about previous works related to the participation of TCLs in frequency control, voltage control as well as combined frequency and voltage control schemes is then provided. Finally, a brief theoretical background about neural networks is introduced.

- Chapter 3: The main objective of this chapter is to develop a mathematical tool for the accurate estimation and prediction of the available control reserves offered by a TCL population. To this aim, the individual model is first evaluated taking into account the variations of the ambient temperature, the frequency, and the voltage. The classical Markov Chain approach for developing an aggregated TCL model is then introduced. The drawbacks of the Markov Chain-based approach for the estimation of

control reserves are outlined. A neural network-based modeling approach is then proposed in this Chapter. The effect of the same variations on the performance of the neural network-based approach is also presented.

- Chapter 4: This chapter provides control methods that allow managing a TCL aggregation as a virtual generator for the provision of primary and secondary control. In particular, the participation of TCLs in primary control is semi-autonomous, which results in an instantaneous response of TCLs to deviations while the communication burden is largely reduced. The exchanged data between TCLs and the aggregator are formulated. Finally, the proposed control methods are validated through various case studies.

- Chapter 5: The control methods developed in Chapter 4 are incorporated within a hierarchical EMS for frequency and voltage control of a microgrid. The optimal coordination of TCLs with other conventional grid resources is investigated. The secondary control is formulated as a PF-based multi-objective optimization to minimize voltage/frequency deviations and the grid operation cost. The proposed control strategy is tested under different case studies to show its effectiveness.

- Chapter 6: In this chapter, the main conclusions of this dissertation are drawn and future work guidelines are identified.

CHAPTER 2   LITERATURE REVIEW

Participation of TCLs as a potential DR reserve in frequency and voltage control schemes has been an active research area. In this chapter, various DR programs, as well as DR beneficial effects on power systems are presented. A general overview of frequency and voltage control and their requirements is then provided. The third part provides a cursory review about previous works related to the participation of TCLs in frequency control, voltage control as well as combined frequency and voltage control schemes. Finally, a brief theoretical background about neural networks is provided.

2.1   Demand Response

2.1.1   Introduction

The concept of DR is increasingly gaining more attention in the world's electricity grids as a propitious pillar of the future energy transition. However, the idea of DR is not new and has been already in place since the seventies. Classical direct load control at the residential level has been used in many countries for maintaining power system relilability. In that period, DR offered the opportunity of load reduction and/or curtailment during periods of contingency or heavy load. However, early DR mechanism was implemented manually and was underutilized namely due to the underdeveloped and expensive communication infrastructure. In 1980, the continuously increasing number of heating and cooling devices had played a major role in the increasing awareness towards the implication of DR and energy efficiency programs especially with the international energy crisis of 1970 and 1980 [23].

Since 1990, the power system has been in the era of transition from a vertically integrated power industry towards an open market system. This has resulted in the reconstruction and deregulation of the electricity market, giving way to the participation of DR along with the conventional resources. In the same vein, many legislative adjustments have taken place in many countries (such us Great-Britain and the United States) aiming to remove unnecessary regulatory obstacles against DR and facilitate its integration in the wholesale electricity market. More recently, DR is redefined as "a reduction in customers' electricity consumption over a given time interval relative to what would otherwise occur in response to a price signal, other financial incentives, or a reliability signal" according to the California Energy Commission [11]. The involvement of DR within electric power industries has been continuously increasing during the last decades resulting in various DR programs [24].

2.1.2 Demand Response Programs

DR programs can be divided into two basic categories [25]:

- price-based programs

- incentive-based programs

Each category can be further divided into subcategories as shown in Figure 2.1.
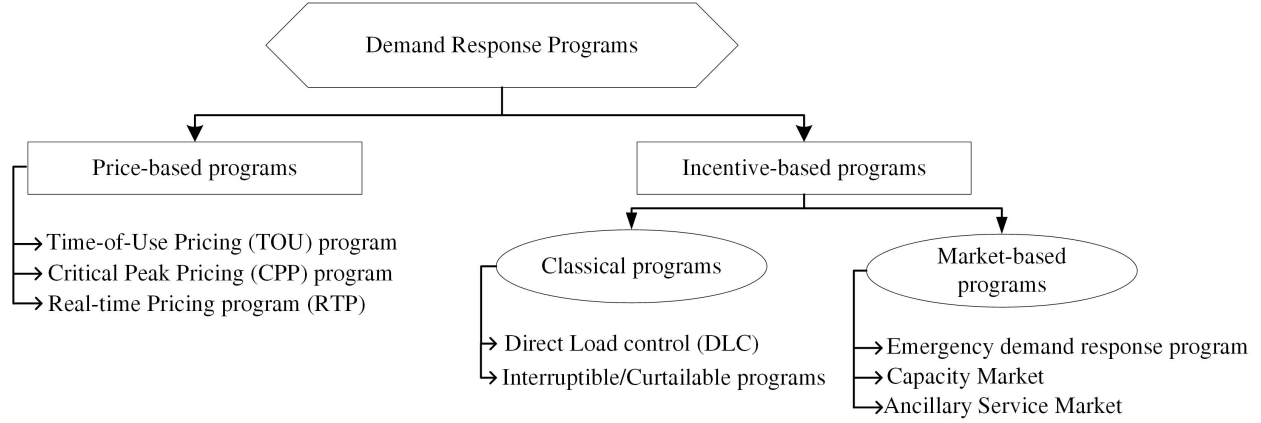
Figure 2.1 Demand response programs

Price-based DR Programs

In price-based DR programs, the energy consumption of each consumer is adjusted in response to changes in the market price of electricity. This program is further split into time-of-use rate (TOU) pricing, critical peak pricing (CPP) and real-time pricing (RTP) [25].

In the TOU pricing, a certain fixed electricity price is allocated to a certain time of the day (e.g. ON-peak, OFF-peak periods), and the consumer knows these prices in advance (day ahead). In contrast, the RTP is based on fluctuating electricity prices on an hourly basis, and consumers are advised about the prices on an hour or day-ahead basis. As for the CPC, it is considered a mixture of TOU and RTP. While its rating structure is analogous to the TOU program, the CPP rates replace TOU rates with much higher prices during specific conditions such us contingencies or very high electricity consumption periods [25].

Incentive-based DR Programs

The second category of DR programs is the incentive-based programs in which customers permit a utility, a grid operator or an aggregator to control its load, usually when the system

reliability is jeopardized or when electricity prices are too high. Enrolled customers receive fixed or time-varying incentive payments or credits in return. Penalties are usually accorded to customers if they fail to respond. A requirement of the incentive-based program is the establishment of an estimation of the customer regular load consumption referred to as the baseline consumption which serves as a reference for measuring and verifying the offered load decrease/increase [24, 26]. There are two subcategories of the incentive-based programs; Classical and Market-based programs.

Classical programs comprise two types; The first type is the direct load control (DLC) in which utilities or aggregators can remotely control the customer equipment such as air conditioners or heating devices on a short notice. This program is mainly intended for residential and small commercial loads. The second type is the interruptible/curtailable program, which is similar to the DLC program, but it is applied to large industrial and commercial customers. In this program, customers who fail to respond might be accorded a severe penalty [24, 26].

The second sub-category of the incentive-based programs is the Market-based program, which in turn is divided into Emergency DR programs, capacity market, and ancillary services market:

- Emergency DR program: In this program, enrolled customers are granted incentive payments in exchange for the measured load decrease during emergency events. There is no accorded penalty in case the customer does not respond, and its participation is voluntary [27].

- Capacity market program: In this program, customers are granted incentives in exchange for a pre-defined load reduction during system contingencies, while penalties are accorded in case of non-response to reduction calls. The Capacity market program can be viewed as an insurance against potential future high peak demand or blackouts during periods of low PV production and high demand for example. In addition to being paid for the provision of the service, customers are also paid for being available even if they are not asked for load reduction [27].

- Ancillary services market: It is an emerging and constantly evolving area [28]. Customers participate in this program by bidding their available reserves in the spot market. Whenever the bids are accepted, selected customers are remunerated for being in the standby state. They are also paid the spot market electricity price in case they provided the contracted ancillary service when required. Although regulation services namely frequency control are the most expensive ancillary service, DR is still under-utilized in this area [15]. This is partially due to the unnecessary legislative barriers which

are today gradually vanishing with the evolving regulatory reforms. These reforms are encouraging the participation of DR and are even allowing them to compete with conventional generating resources [27]. It is noted that for a realistic implication of DR in the ancillary service market, the technical requirements which vary depending on the type of the provided service should be taken into account. For instance, smart metering and the ability to respond very fast to system operator instructions might be necessary in the case of primary and secondary frequency control [26]. The work presented in this thesis fall under the category of ancillary services market DR program.

2.1.3   Demand Response benefits

The real implementations of DR programs have been majorly focusing on peak-shaving or peak load reduction. Their technical and economic effectiveness has been justified through various field programs such as the SmartAc project of the Pacific Gas and Electric Company (PG&E) or Ontario's demand response programs, etc. More recently, increasing attention has been dedicated to the participation of DR in the provision of regulation services such as frequency control. The participation of DR in these control areas is considered more alluring mainly because these services require shorter response duration and fewer response times as compared with peak load reduction service that requires a response many hours in a day with longer response time [15].

As the focus of this work is on the provision of frequency and voltage control services, some of the advantages related to the implication of DR in these services are briefly presented in the following. In general, DR offers various potential benefits at different levels that can be societal, economic, technical or environmental [15, 27]:

- Societal level: The societal benefits are basically related to the active participation of consumers in electricity markets, which allows them to receive payments or credits that certainly lower their electricity bill. Their participation in regulation services is of exceptional interest because, as discussed earlier, they are the most expensive services, and therefore, the most rewarding ones.

- Economic level: DR is expected to have a favorable impact on the overall electricity market price. From one part, DR reduces the need for running or installing new expensive generators such as the quick start units. From another part, DR helps in dividing load mismatches with other generators implying lower power production from conventional generators. These will undoubtedly reduce the overall electricity cost.

- Technical level: DR involvement in regulation services increases the available reserves

for regulation and therefore limits the risk of outages and their impact on the grid, which enhances the reliability and stability of the system. Furthermore, DR can reduce the grid losses, especially when contributing to voltage control.

- Environmental level: DR contributes to reducing Greenhouse gas emissions in two ways; First, DR helps in better integrating renewable resources in the grid as it contributes to tackling fluctuations resulting from high renewable sources penetration. Second, the integration of DR results in reduced emissions and natural resources conservation for two reasons. From one hand, the need for installing fast-start generators fueled mainly with oil or Diesel is reduced. From the other hand, when the loads share the regulation task with the existing fossil-fueled generators, the reliance on the conventional generators is reduced.

2.2 Frequency and Voltage Control of a Power System

2.2.1 Introduction

Ancillary services are the set of tools used by grid operators to maintain the balance between generation and demand. Frequency and voltage are accurate indicators of generation-consumption imbalance in a given power system. Deviations in frequency and voltage must be tackled within short periods. At the customer side, electric motors or electrical appliances are constructed to operate within certain restricted allowable margins of voltage and frequency. Otherwise, the performance of these appliances is affected and they may be prone to damage in some cases [29, 30]. Similarly, frequency and voltage must be kept within specific ranges to prevent the generators connected to the grid from going offline which can ultimately result in system collapse and blackout [31]. Furthermore, maintaining voltages at different nodes within their permissible limits ensures an efficient system operation with reduced line losses [29]. Therefore, an appropriate control strategy is crucial for maintaining frequency and voltage within the admissible ranges.

Generally, two typical approaches, namely the centralized and decentralized approaches, are adopted to control voltage and frequency of power systems. In the fully centralized control, a central controller is responsible for measuring and collecting system's data, processing them and accordingly delivering control decisions [3]. While this control allows clear observability and precise controllability of the whole system, it requires a reliable infrastructure due to the massive amount of exchanged data among the central controller and other units. In the fully decentralized approach, each unit is governed by its own local controller, and therefore each unit takes control decisions individually without any dependence on or communication

with other units. Combining these two approaches gives rise to the hierarchical control structure [32].

Generally, the hierarchical control structure of a power system is composed of 3 layers: primary, secondary and tertiary control [2–4]. Each control layer has a particular role with specific requirements, as will be detailed in the following.

2.2.2 Primary Control

Primary control constitutes the first defense line of the system and has the fastest response (within seconds). It is of great importance as it is responsible for maintaining the stability of the system following large generation-consumption imbalances. Taking the example of Great-Britain, the primary reserve response must be available within a maximum of 10 seconds and upheld for around 20 seconds further. Primary control is typically performed locally by synchronous generators with no reliance on communication whenever a disturbance is locally sensed. The voltage control is typically achieved by the automatic voltage regulator (AVR) that continuously adjusts the excitation in order to maintain a constant voltage level [29]. As for the frequency control, it is achieved by the turbine-governor control system to maintain the frequency at its desired value.

The control of frequency and voltage can be obtained using the droop-based control method. The idea of droop control is to link the active and reactive power variation of the generator output to the variations of frequency and voltage. The linear relation is the most common in the literature. In case of systems that are characterized by a high X/R ratio, the control of frequency is accomplished by controlling the active power, while the voltage control is realized by the control of reactive power flow. An example of typical P-f/Q-V droop characteristics is illustrated in Figure 2.2 [32].
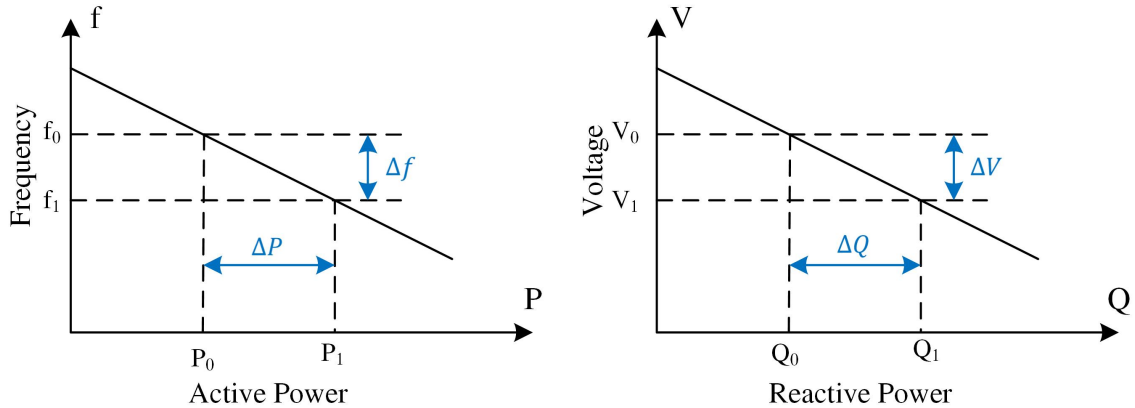
Figure 2.2 Droop Characteristics

On the other hand, in resistive systems (low X/R ratio) the correlation is strong between voltage and active power from one hand and between frequency and reactive power from the other hand. In this case, P-V/Q-f droop control can be applied [32]. For example, in [33] such droop control is applied to a weak LV network-based microgrid.

An important feature of the droop characteristics is its slope that is referred to as the droop coefficient K (K_P in case of P-f droop and K_Q in case of Q-V droop). For example, if K_P is equal to 2 p.u./Hz, then if the frequency decreases by 0.2 Hz, the active power of the generating unit increases by 0.4 p.u.. In case one or more generators are connected in parallel to the power system, the droop coefficients ensure a stable load sharing between generators. To better illustrate the idea, two generators G1 and G2 are considered with initial power outputs P1 and P2 and droop coefficients K_1 and K_2, respectively. Upon a disturbance, G1 and G2 react by changing their power outputs to P_1' and P_2', respectively. Thus, each generator, with respect to its droop, picks up a certain amount of load that is equal to [34]:

$$\Delta P_1 = P_1' - P_1 = K_1 \Delta f \tag{2.1}$$

$$\Delta P_2 = P_2' - P_2 = K_2 \Delta f \tag{2.2}$$

Thus, in general:

$$\frac{\Delta P_1}{\Delta P_2} = \frac{K_1}{K_2} \tag{2.3}$$

Therefore, if the droop coefficients are set almost equal, then each generating unit will change its output power in proportion to its size (rating).

The aim of the primary control is only to stabilize frequency and voltage and prevent them from further drifting, but it cannot bring them back to their nominal values, especially in case of severe deviations. Therefore, another control layer is needed to achieve this goal, which is the secondary control [32, 35].

2.2.3 Secondary and Tertiary Control

The secondary control aims to eliminate the residual frequency and voltage deviations that persist after the action of the primary controller. The main goal of the secondary control is to bring back frequency and voltage close to their nominal values. In the case of large inter-connected systems, it additionally targets the restoration of tie-line flows to the contracted amounts. The optimization of the economic operation can also be a goal of this control layer. Compared with the primary control, the secondary control has a slower dynamic response (approximately acts 30 seconds after the event occurrence) and therefore it is usually cen-

tralized as enough time is available to perform processing and complex computations by the system operator as well as to have high-level coordination of the units. The objectives of this control level are generally achieved by the allocation of new optimal set-points for the generators.

As for the tertiary control, it is the slowest control level (operation in minutes to hours) and is performed by automatic or manual changes in the set-points of the participating generators. It is designed to restore the secondary reserves in order to have a system that is ready to respond to new deviations. The tertiary control mainly deals with the long-term system-wide coordination of the system. In the case of a microgrid, this control appears in the form of optimizing the power flow between the considered microgrid and the main grid or among various microgrids. It is noted that the tertiary control is not needed in the islanded operation of microgrids. [36, 37].

It is noted that the time frames related to these control levels differ from a system to another, and there is not a common consensus on specific values [3].

It can be concluded that these control levels differ in terms of the granted role, response speed, the infrastructure requirements (specifically the communication), and time interval during which they keep operating.

2.3 TCLs Participation in Frequency and Voltage Control

2.3.1 Thermostatically Controlled loads

Thermostatically Controlled Loads (TCLs) are a potential DR reserve and are considered as an attractive resource for participation in electricity markets by providing control reserves [38]. In general, TCLs can be defined as electric appliances having the role of maintaining the temperature within a predefined deadband through their switching ON/OFF capability. Examples of such appliances include refrigerators, heat pumps, space heaters, air conditioners, water heaters, etc. TCLs are regarded as an attractive means for the provision of ancillary services for many reasons illustrated in detail in Chapter 1.

In brief, TCLs are already ubiquitous in large numbers and their number is expected to grow significantly in the coming years [14]. Furthermore, the inherent flexibility of TCLs allows them to be managed without affecting customer comfort. In fact, TCLs have the function of keeping the temperature within a predefined deadband through their switching ON/OFF capability. For a heating device for example, when the temperature reaches the upper-level limit the device is automatically switched OFF while switching ON occurs when the temperature reaches the lower-level limit. Therefore, in case a power reduction is needed,

a TCL in ON state can receive an external signal to turn it off for a specific time while ensuring that the temperature is still within the permissible range during that time [15]. Moreover, TCLs are considered as a cost-effective and fast-responding reserve which makes them suitable even for the provision of ancillary services that require a very fast response such as primary frequency control. These two characteristics are generally what makes TCLs outperform conventional generators [15].

All these features make TCLs a suitable and alluring resource to be exploited in services such as frequency and voltage control which are challenging economically and technically, especially in terms of response speed.

2.3.2 Aggregated TCL Models

In control applications, the concept of aggregation involves combining a large number of units into a single control entity that is much simpler and easier to handle. This aggregated unit is also used to figure out how the constituting smaller units will respond to instructions or events that affect the aggregation [39]. More specifically, the aggregation can be applied to many small-scale DERs to represent them as a single controllable power resource that can be used by different power system actors such as the system operator.

There has been an interest in defining an aggregated model for a population of TCLs. This helps to better study the effect of a large number of TCLs on the dynamic behavior of the power system. In fact, the power consumption of a single TCL is in the order of a few kW. Therefore its contribution to the grid demand side is negligible. Considering that the summation of the power of thousands of TCLs can be in the order of MWs, the collective behavior of a population of TCLs can be comparable to the output power of a generator. Furthermore, a few TCLs cannot participate in ancillary service markets because these markets usually define a minimal threshold for accepting a power bid offer. For example, in the case of the PJM, a minimum of 1 MW is required to be accepted primarily in the bid selection process [40].

Moreover, an accurate aggregated model can facilitate the bidding procedure especially with the ancillary service markets related to frequency control as it requires very short-term bidding (e.g. 5 minutes in the case of PJM) with high resolution. In this case, the aggregated model can enable a fast and accurate estimation as well as a prediction of the available flexibility to offer for control purposes. An accurate very short-term prediction of the available control reserve is of great importance as it allows to avoid penalties due to the inability to deliver the predicted reserve amount when needed especially in the case of reserve overestimation.

Another interesting motivation towards aggregation is the resulting reduced complexity, smaller execution time in the context of simulations and lower memory usage when adopting an aggregated model of a TCL population. As the number of TCLs is continuously increasing, considering an individual model for each TCL is a time-consuming and computationally expensive task that is not practical for applications such as real-time simulation and frequency control where time efficiency is a critical factor [41].

In conclusion, formulating an accurate yet straightforward aggregated model of a TCL population is of great importance to reduce the computational complexity stemming from the individual modeling of hundreds or thousands of TCLs. Furthermore, a simplified aggregate TCL model is needed for control system applications and to estimate and predict the amount of the control reserve that can be offered by the TCL population.

In the literature, there exist various aggregation models of TCLs. For example, a TCL cluster has been modeled as an energy storage unit in [42], and as a virtual power plant in [43]. In [44], coupled Fokker-Planck equations have been solved in order to obtain a stochastic aggregated load model. A state queuing model has been developed in [45] considering modeling uncertainties. Input-output models have also been proposed as in [46]. Another prevalent class of aggregated TCL model is the state-bin transition model that describes the dynamic behavior of TCLs as a Markov chain process as has been proposed in [47–50].

2.3.3 Control Strategies for Frequency and Voltage Control by TCLs

TCLs participation in frequency control

Traditionally, TCLs have been extensively employed in peak shaving and peak load reduction. More recently, the focus has been given to TCLs provision of reliability services with a major focus on their employment in primary frequency control. The Centralized control strategy is a common approach that is based on a DLC mechanism [50–56]. In this framework, a control center usually acquires data from TCLs and sends back control decisions that can be direct ON/OFF commands or new temperature operating set-points. Although the centralized approach is easily implementable and provides accurate responses, various investigations underscore its futility as it is mainly affected by communication quality. In fact, it has been argued that real-time control systems are unreliable for being subject to communication impairments and delays while requiring an expensive infrastructure, especially when the number of TCLs is considerable [18, 43].

To overcome these issues, fully decentralized strategies have been proposed in various studies as in [57–61]. In the decentralized approach, each device is governed by the control deci-

sion of its own local controller without interacting with other controllers in the grid. For example, in [60], a population of fridges has been considered for stabilizing the frequency. Each fridge is equipped with a local controller that regulates the upper and lower switching temperatures linearly with the frequency deviation. The technical and economic feasibility of providing primary frequency control by switching ON/OFF residential appliances based on local frequency measurements using a smart meter has been experimentally demonstrated in [61]. Although the decentralized strategies have proven to be operational in power system applications while preserving customer comfort and reducing communication cost, they fail to manage the overall system operation and achieve global system-level objectives since local controllers may conflict against each other to achieve the local desired goal. In fact, it has been argued that in fully decentralized schemes, the aggregated response of a TCL population usually results in either over or under-response, which makes it difficult to reach a system-level set-point. Consequently, this situation raises the need for a higher coordinating control level [18].

To bridge the gap between centralized and decentralized approaches, hierarchical control strategies have been proposed as a compromise between centralized and decentralized approaches. The effectiveness of the hierarchical control strategy has been proved in many recent studies [18, 19, 62–64]. The principle of this approach is that control parameters are regularly sent from a central unit to TCLs, but the local controller of each TCL acts autonomously. Unlike the centralized control, these control parameters (e.g. trigger frequencies) are not direct control decisions but rather represent a sort of instructions that will guide the local controller in the choice of its control decisions. The updates of control parameters occur at time intervals that are longer (minutes to hours) than the actual response time scales (from seconds to minutes) implying that no real-time communication is needed between the central unit and TCLs. This principle of operation is referred to as 'semi-autonomous' operation in the literature. As compared to the decentralized scheme, the control parameters are issued from a central unit overseeing the resources (TCLs), which implicitly allows reaching global system-level coordination without any need of communication between TCLs. For example, in [19], a two-level control strategy is proposed using a semi-autonomous operation of TCLs for primary and secondary frequency control in the Great Britain power system. In [65], [66] and [67], the autonomous operation of TCLs is achieved through trigger frequencies dispatch, which guarantees a fast response and a low communication burden.

Although these approaches almost have the same operation principle, what differentiates between them is the definition of control parameters. These parameters are of great importance as they allow to achieve system-level coordination among resources, while having the responsibility of prioritizing the response of devices, taking into account short cycling effects,

minimizing the number of ON/OFF switching of each device, etc.

As for the secondary frequency control, the participation of TCLs is similar to the classical DR strategies in which a group of loads is modeled as a negative generation unit [10,22]. A change in the collective power consumption of TCLs can be performed either by direct ON/OFF switching or by changing the set-point temperatures. Various methods have been proposed in the literature and they differ mainly in terms of their methodology adopted for determining the amount of load increase or decrease required from a TCL population as well as the selection of participating TCLs. For example, in [68], a secondary frequency control strategy has been experimentally tested where refrigerators receive control commands to switch their status to OFF-state. TCLs with higher temperatures are prioritized. The appliances are gradually switched OFF until the amount of power required by the central controller is reached. An adaptive refrigerator model has been used to predict which appliances will stay longer in the OFF-state in order to maintain the envisaged load reduction [63].

TCLs participation in voltage control

In this part, we review some of the presented works in the literature in which the relation between TCLs and voltage control is highlighted. Although there are various studies about TCLs provision of voltage control, this application has not gained the same interest as the frequency control. Concerning the relation between TCLs and the voltage, one should note that TCLs are voltage-dependent loads as described by the component-based load modeling approach [69]. This implies that a TCL power output and duty cycle are affected following a voltage change [70]. It is to be noted that there are two main categories of TCLs: The first category is composed of resistive TCLs such as electric water heaters that consume only active power. The second category is that of TCLs that are equipped with induction motors (e.g. heat pumps, refrigerators, HVACs, etc) implying that the reactive power consumption is existent along with the active power as discussed in very few works [16,71].

Although many works have considered the voltage dependency of TCLs, this feature has not been used for voltage control purposes, but rather for affecting the aggregated power consumption of TCLs which is of interest in applications such as load following. These approaches rely on the principle that, if the power output of TCLs is affected by voltage variations, then one can control the power consumption by appropriate control of voltage at system buses. For example, in [71], a tap changer is used to control the voltage at the point of common coupling in order to control the aggregated power consumption of TCLs. In [72], voltage-dependent loads including TCLs have been used to regulate the frequency. Reactive power compensators are employed to control the magnitude of supply voltage, and

consequently, the active power consumption of voltage-dependent loads including TCLs is changed which further supports the frequency regulation.

Some works in the literature have employed resistive TCLs for voltage control. This is exclusively possible in case of distribution networks where the R/X ratio is high entailing a coupling between active power and voltage [73]. For example, the work presented in [74] concluded that the coordination between demand response and distributed generators (DGs) in distribution networks could reduce the cost of voltage control. To this end, the problem has been cast in the form of a centralized optimization to minimize voltage control costs related to tap changers, DGs and demand response, and is subject to various constraints among which is maintaining voltage profile within acceptable ranges. In [71], TCLs are considered as a 'voltage controlled reserve' for participating in a short-term voltage control scheme. Two control logics have been considered for controlling TCLs; TCLs can either be switched ON/OFF based on local voltage measurements, or their set-point temperature is modified linearly with the voltage variation. The majority of works that considered reactive power consumption fall under the category of load curtailment. In [75], loads have been curtailed as part of an emergency DR program in order to participate in a real-time voltage control scheme in coordination with tap changers. Considering the impact of both active and reactive powers on voltage profile in distribution networks, load sensitivity matrices have been used to study the effect of the load variation on the voltage [75]. Optimization problems are usually formulated as in [76] and [22] to determine the optimal active and reactive powers to be adjusted by load manipulation. However, the demand response model used in these works is usually very general as no specific model for TCLs is developed, but rather it assumes that specific amounts of loads are curtailable at certain times. In general, the reactive power consumption of TCLs is usually ignored, and only a few studies (e.g. [16]) have considered this feature.

TCLs participation in frequency and voltage control

As discussed earlier, there are various control strategies proposed in the literature integrating TCLs in frequency or voltage regulation services. However, providing each service separately may result in unfavorable effects as objectives may be conflicting. This effect has been partially highlighted by [21] through simulation results in five real distribution grids. It concluded that despite the use of voltage regulators, load-based frequency regulation increases the risk of violating voltage limits. This risk is more likely to increase in the absence of voltage regulators. Let alone that even with voltage regulators, the exact voltage value is not necessarily assured in all nodes [77]. The effect of voltage unbalance mitigation on the

frequency has been assessed in [16] concluding that voltage regulation using TCLs results in un-intentional over/under frequency. Therefore, using TCLs for both frequency and voltage control within the same control strategy is of great interest as it limits the unfavorable effects while fully leveraging the full potential of TCLs. Only a few studies have presented a framework for both frequency and voltage control. In [20], a TCL-based hierarchical control strategy for secondary frequency control has been proposed using an optimal power flow approach subject to distribution network constraints. However, the proposed approach is fully centralized and neglects communication requirements, hence cannot be extended to the primary control. A control strategy for combined voltage and frequency control by the coordination of distributed energy resources (DERs) and DR has been proposed in [22]. However, the paper has not distinguished between primary and secondary control levels, and the participation of DR has not been prioritized i.e. only confined to cases of heavy loading.

2.4   Neural Networks

In general, The dynamic behavior of a TCL population depends on various internal and external parameters such as the temperature setting, thermal parameters, the ambient temperature, deadband, etc. It would be of interest to express the aggregated power consmption of a TCL cluster as a function of some of these time dependent parameters. Therefore, the aggregation of a TCL population can be formulated as a function-fitting problem.

The function-fitting generally applies to the modeling of complex relations between input-output data, and then use the approximated function to predict outputs based on new given input data. Function-fitting problems can be solved by a variety of techniques ranging from very simple approaches such as linear regression to more advanced ones such as the neural networks. In fact, neural networks belong to the family of machine learning algorithms that have been receiving increasing attention over the past years in a variety of fields. Neural networks have been widely used in classification and prediction applications, and have shown to be a potent and robust computational tool. In particular, with relation to the function-fitting context, a neural network can be viewed as a function that attempts to fit the input-output data while capturing the underlying most complex and non-linear relations between them with a high accuracy [78].

A neural network, as its name suggests, consists of a set of interconnected elements called neurons that work in parallel. Inspired by the functioning of a human brain, a neural network can learn how a complicated process works with no need to program it explicitly. It learns by itself based on a given set of inputs and their associated outputs (targets) [79]. Training a neural network relies on finding an adequate mapping between given inputs and outputs,

and the trained network can be used later to predict the outputs based on the new input information [80, 81].

The typical architecture of a feed-forward neural network is illustrated in Figure 2.3. In general, the architecture is composed of inputs, intermediate layers called hidden layers and an output layer. Each intermediate layer consists of neurons each considered as a processing unit [79, 80].
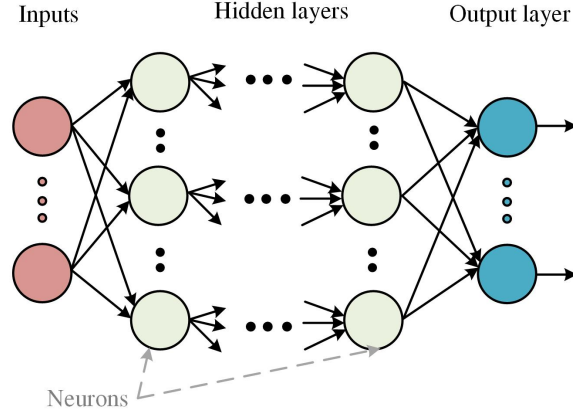
Figure 2.3 Typical neural network architecture

To better understand how inputs-outputs are related, a two-layer feedforward neural network is considered as shown in Figure 2.4.
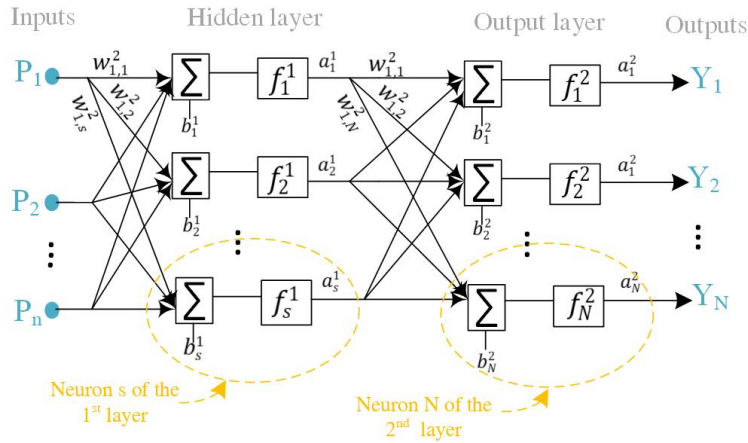
Figure 2.4 A two-layer feedforward neural network structure

The neural network has 'n' inputs, 'N' outputs, 's' neurons in the first layer and 'N' neurons in the second layer (output layer). In general, the output of each layer 'j' is a vector $(a_i^j)_{1 \leq i \leq p_j}$

where p_j is the number of neurons in the jth layer. Each component a_i^j of the vector a^j denotes the ith output of the neuron 'i' of the jth layer [81].

Each neuron has weights, a bias value and a transfer function; The ith neuron of the jth layer has [81]:

- Input weights vector $(w_k^j)_{1 \leq k \leq p_{j-1}}$ where p_{j-1} is the number of neurons of the preceding layer (if j=1, p_{j-1}=n)

- Bias b_i^j

- Transfer function f_i^j

Therefore, considering a layer 'j', all input weights vectors of each neuron can be collected in one matrix denoted by w^j, and similarly all bias values and transfer functions are collected each to form vectors b^j and f^j, respectively. Based on these notations, each layer comprises a weight matrix, a bias vector and a transfer function, and the output of the 1st and the 2nd layers can be expressed respectively by (2.4) and (2.5),

$$a^1 = f^1(w^1 p + b^1) \tag{2.4}$$

$$a^2 = f^2(w^2 a^1 + b^2) \tag{2.5}$$

It is noted that superscripts denote the number of the layer. The transfer functions can be a sigmoid, a linear function, a hard-limit, etc. In this work, the hidden layer transfer function is a sigmoid function while the output layer transfer function is linear. Weights and biases are not constant but are rather adjusted within the process of training the neural network. In fact, training a network refers to the continuous adjustment of weights and bias values throughout the training process using input-output pairs in order to achieve a desired task with a satisfying performance. The desired task is to solve a fitting problem using the neural network. In other words, throughout the learning process, the weights and biases are adjusted in a way that minimizes an error that is, similar to the conventional fitting problems, the summation of the squares of the differences between the correct output and the calculated neural network output. Many optimization techniques can be used for this purpose which differ namely in terms of speed, accuracy and required memory. Examples are the Levenberg Marquardt, Gradient descent, Conjugate gradient, etc. In this work, the Levenberg Marquardt algorithm is used for training the network. This is an algorithm which is commonly used and is known for its robustness [81].

2.5 Conclusion

In this chapter, a review on DR, its programs and benefits have been provided accentuating the importance of DR in assisting the operation of electric grids both technically and economically. The provision requirements of frequency and voltage control have been also reviewed. The main TCL aggregated models used in the literature are presented. Furthermore, some of the previous studies that have involved TCLs in the provision of frequency and voltage control has been discussed. It is found that the majority of works have majorly dealt with the participation of TCLs in frequency control applications, while less attention has been given to their participation in voltage control. It is also revealed that although the integration of TCLs in both frequency and voltage control within the same control framework is of great interest, only a few works have dealt with it. Finally, a brief theoretical background about neural networks is provided which will serve as a basis for estimating the available control reserves offered by TCLs.

CHAPTER 3   AGGREGATED TCL MODEL FOR ANCILLARY SERVICES

The individual TCL model is presented and studied under the variation of various factors, namely the ambient temperature, frequency and voltage. A common state-bin aggregated model is then presented which serves as a basis for evaluating the available control reserves. Two approaches are used for evaluating the available reserves; The first is the classical Markov-Chain approach and the second, which is proposed for the first time in this thesis, is based on neural networks. The performance of both approaches is then compared in terms of prediction accuracy.

3.1   Individual TCL Model

3.1.1   Thermal Dynamics

The first step prior to including TCLs in demand response is to study the dynamic thermal behavior of a single TCL. A TCL can operate in heating or cooling mode and can be in ON-state i.e. consuming power, or in OFF-state where no power is consumed. A common discrete-time model to describe the temperature evolution of an individual TCL 'i' is as follows [82]:

$$T_i^{k+1} = e^{\frac{-h}{RC}} T_i^k + \left(1 - e^{\frac{-h}{RC}}\right)\left(T_a^k \pm m_i^k.R_i.COP_i.P_i\right) + \omega^k \tag{3.1}$$

where signs - and + are used for cooling and heating modes respectively, T_i (°C) is the temperature of the heated/cooled zone and T_a (°C) is the ambient temperature; C and R are the thermal capacitance (kWh/°C) and thermal resistance (°C/kW) respectively; h is the sampling period and k denotes the actual time step; m_i is the switch status (i.e. ON or OFF status); COP is the coefficient of performance; ω is the white noise and P_i (kW) is the electrical power consumption of the TCL.

In the majority of studies, the electrical power consumption of a TCL is considered equal to its rated output power for the sake of simplification which is the power specified by the manufacturer. However, in more accurate studies, TCLs are considered as voltage and frequency dependent devices and therefore their power consumption depends on the actual voltage and frequency [70]. Furthermore, when the TCL is equipped with an induction motor, its reactive power consumption must be considered as well. Therefore, the active and reactive

power consumption of a TCL can be respectively approximated by [69, 83, 84]:

$$P_i = P_{rate,i}\left(\frac{V}{V_0}\right)^{n_p}(1 + k_p(f - f_0)) \tag{3.2}$$

$$Q_i = Q_{rate,i}\left(\frac{V}{V_0}\right)^{n_q}(1 + k_q(f - f_0)) \tag{3.3}$$

Where factors n_p and n_q are the voltage dependency parameters; k_p and k_q are the frequency sensitivity parameters. Practically, the voltage dependency parameters are deduced from the ZIP coefficients (Z: constant impedance, I: constant current, P: constant power) as reported in [70], and can be expressed as follows:

$$n_p = \frac{2 \times Z_p + 1 \times I_p + 0 \times P_p}{Z_p + I_p + P_p} \tag{3.4}$$

$$n_q = \frac{2 \times Z_q + 1 \times I_q + 0 \times P_q}{Z_q + I_q + P_q} \tag{3.5}$$

The frequency sensitivity parameters are obtained through measurement of frequency sensitivities of some typical loads, and can be approximated with reference to [84]. It is noted that in case the power factor of a TCL is known, its reactive power can be simply deduced based on the active power consumption as follows [16]:

$$Q_i = \left(\frac{P_i}{\cos(\Phi)}\right)^2 - P_i^2 \tag{3.6}$$

where $\cos(\Phi)$ is the power factor.

The natural operation process of a single TCL is illustrated in Figure 3.1. The role of a TCL is to keep the temperature of the heated/cooled zone within a deadband around a pre-defined temperature set-point; i.e. the temperature is kept between an upper and lower bound temperature. When operating in heating mode, whenever the temperature reaches the upper-bound, the device is turned OFF, and consequently, the temperature will keep on decreasing until it reaches the lower-bound temperature. Reaching the lower-bound temperature triggers the TCL to be turned ON again with the temperature increasing until it reaches the upper-bound limit, and so on. The switching dynamics of a single TCL which is referred to as thermostat control can be described by:

$$m_0(k+1) = \begin{cases} 0 & if\ T^{k+1} > T^+\ ; \quad T^+ = T_{set} + \frac{\delta_{db}}{2} \\ 1 & if\ T^{k+1} < T^-\ ; \quad T^- = T_{set} - \frac{\delta_{db}}{2} \\ m_0(k) & otherwise \end{cases} \tag{3.7}$$

where m_0 is the natural switch status. T_{set} is the set temperature and, δ_{db} is the temperature deadband. T^+ and T^- are the upper and lower temperature bounds, respectively. The user's comfort is guaranteed as long as the temperature is within the deadband.
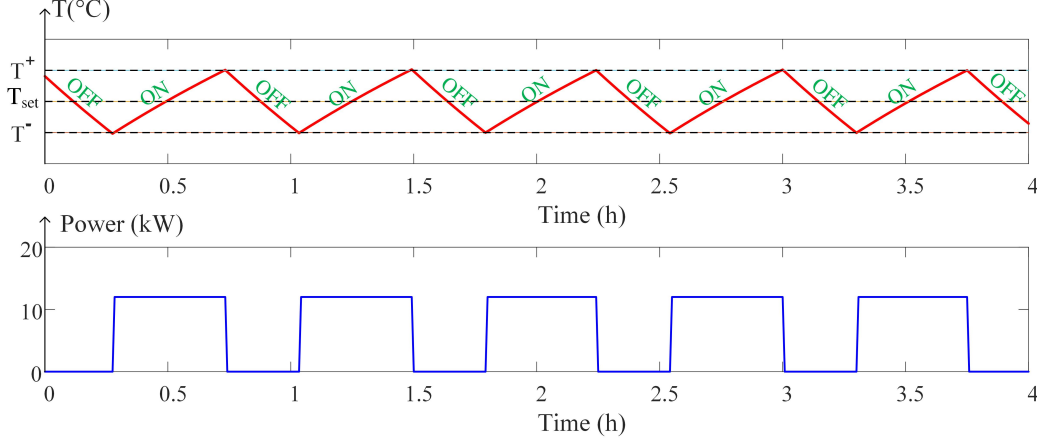
Figure 3.1 Heating device natural switching.

3.1.2 Power Consumption of a TCL Population

Based on the individual model of each TCL, it can be seen that many factors affect the temperature evolution as well as the power consumption over time. In particular, given a population of TCLs with pre-defined parameters considered as unchanged over time (i.e. thermal capacitance, thermal resistance, set temperatures, rated power and deadband), the thermal dynamics depend on the ambient temperature, voltage and frequency. As our main interest is on the power consumption over time, the effects of the ambient temperature, as well as the voltage and frequency will be analyzed in this section.

Ambient Temperature Factor

The ambient temperature is a continually changing parameter, and its fluctuation is in the scale of minutes. Therefore, an analysis of its impact on the dynamic behavior of a single TCL as well as on a cluster of TCLs is provided in the following.

To this aim, 3 TCLs in heating mode with the same parameters and initial conditions are simulated at three different ambient temperatures of 3 °C, 4 °C and 5 °C. The temperatures, as well as the power profiles for each case are illustrated in Figure 3.2.

It can be seen from Figure 3.2 that the variation of the ambient temperature affects the dynamic behavior of a TCL as temperature and consumption power profiles are affected.
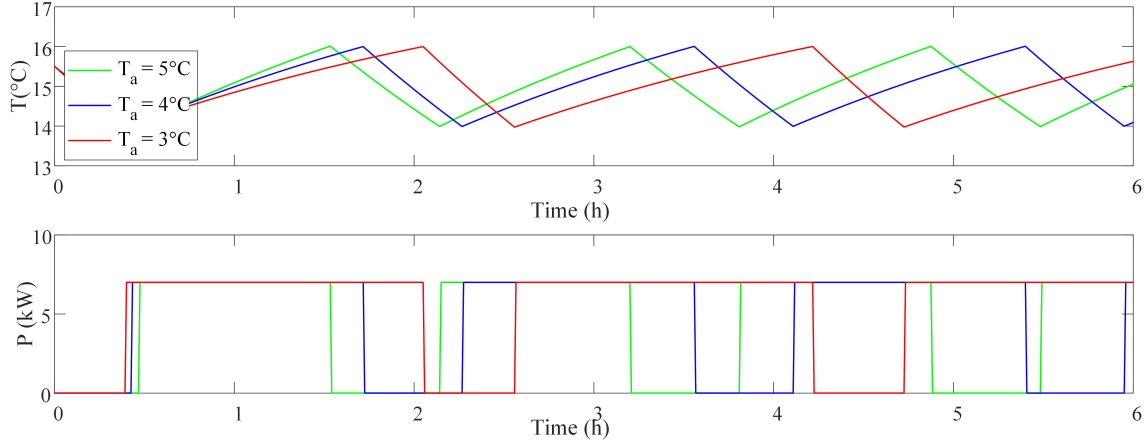
Figure 3.2 The effect of ambient temperature on TCLs' temeperature and power consumption.

Whenever the ambient temperature increases, the TCL operates at shorter time-periods with the same amount of consumed power. Observing the slope of the temperature curve of each case, it can be noticed that the rate of change of the temperature increases with the increase in the ambient temperature. By looking at the duty cycles of the temperature and power profiles shown in Figure 3.2, it is generally seen that at lower ambient temperature, the time duration spent by a TCL in ON state increases while the frequency of the signal decreases. Therefore, given a fixed period, the energy consumption decreases when the ambient temperature increases.

To evaluate the effect of the ambient temperature on the power consumption of a group of TCLs, a heterogeneous population of 1000 TCLs is considered. Parameters used to simulate the population are shown in Table 3.1. To account for randomness and heterogeneity in a TCL population, the majority of parameters are randomly chosen based on a uniform distribution. It assumed that initially, 50% of the population is in ON-state while the other half is in OFF-state. The population is first simulated at an ambient temperature of 3 °C. The same population is then simulated under the ambient temperatures of 4 °C and 5 °C. The power consumption profile for each case is presented in Figure 3.3.

It is seen from Figure 3.3 that the power profile of the TCL population is strongly affected by the ambient temperature. Even a temperature increment of 1°C can induce a significant difference in the overall power consumption. Generally, in heating mode, the power consumption is larger at lower ambient temperatures.

To conclude, the ambient temperature has a strong effect on the individual dynamic behavior of a TCL as well as on the collective behavior of a TCL population.
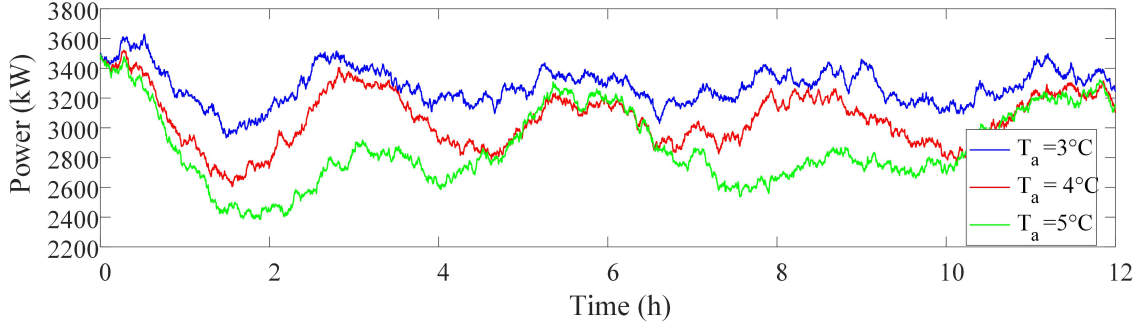
Figure 3.3 The effect of ambient temperature on the active power consumption of a population of 1000 TCLs.

Table 3.1 TCL simulation parameters taken from [65]

Parameter	Range	Distributoin type
T_{set}	15~20°C	Uniform distribution
C	$8{\sim}12kWh/°$C	Uniform distribution
R	1.5~2.5°C/kW	Uniform distribution
δ_{db}	2°C	-
P_{rate}	6~8 kW	Uniform distribution
COP	3	-

Voltage and Frequency Factors

TCLs are voltage and frequency dependent loads as described by equations (3.1), (3.2) and (3.3). Therefore, it is expected that voltage and frequency variations have an influence on both the dynamic behavior of an individual TCL and the collective behavior of a TCL population.

To better understand this fact, the temperature and power profiles of a single TCL are simulated under different voltage levels. The voltage dependency parameter is set to 0.51 [16]. Simulation results are shown in Figure 3.4.

The voltage affects both the temperature and the power profiles as can be seen in Figure 3.4. At a higher voltage, the TCL remains a shorter time in the ON-state, but consumes a higher amount of active power. Due to an increase in the voltage, the energy consumption of a TCL in ON state increases, and the frequency of the power profile increases.

To investigate the effect of the voltage on the energy consumption of a TCL population, a number of 1000 TCLs is considered with the parameters illustrated in Table 3.1. Initially, half of the population is in ON-state, while the other half is in OFF state and the voltage
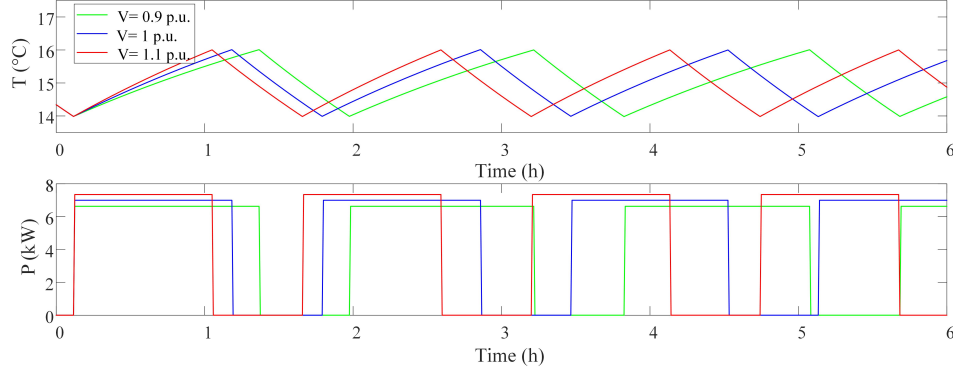
Figure 3.4 The effect of voltage variation on the active power consumption of a single TCL.

dependency parameter is set to 0.51 [16]. The variation of the overall power consumption of the TCLs during 6 hours is shown in Figure 3.5
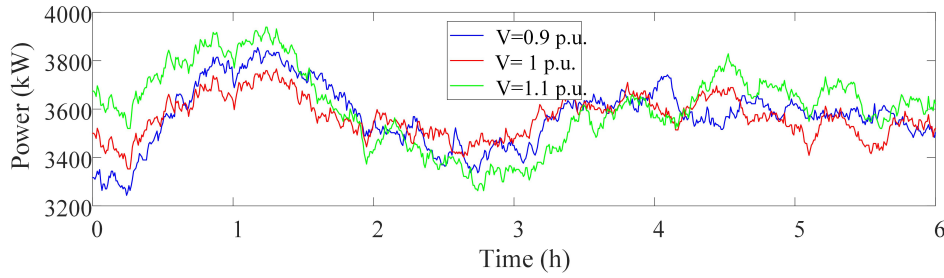
Figure 3.5 The effect of voltage variation on the active power consumption of a population of 1000 TCLs.

Overall, Figure 3.5 shows that the active power profile of the population is affected by the voltage levels. It can be concluded, by looking at the first 2 hours, that smaller voltages result in a more prolonged ON-state operation with lower active power consumption. Furthermore, it is seen that if the voltage level is small at a given period, there will be an increased power consumption in the following periods. This is confirmed by comparing the power consumption during the time interval [0, 2 h] with that of the time interval [2h, 4h]. The same effect can be seen by comparing the power during the intervals [2h, 4h] and [4h, 6h].

It is noted that frequency variations similarly affect the active power profiles exactly as the voltage effect.

In sum, the ambient temperature, the voltage and the frequency have a noticeable effect on the active power consumption of TCLs. Therefore, It is essential to consider the voltage and frequency dependency of TCLs, especially in a microgrid that is frequently subject to

large deviations of voltage and frequency depending on its operation mode i.e., islanded or grid-connected.

Combined Effect of Ambient Temperature, Voltage and Frequency Variations

To further evaluate the effect of ambient temperature, voltage and frequency on the active power consumption of a population of TCLs, a simulation using 2000 TCLs with parameters listed in Table 3.1 is conducted. The control interval and the simulation time step are set to 2 minutes and 30 seconds respectively. $k_P = 1.5$ and $n_p = 0.5$ are used to describe the voltage and frequency dependence of TCLs. The Temperature variations are taken from the weather station ISEP/IPP with reference to a real measurement site with a resolution of 5 minutes [85]. Voltage and frequency variations are generated randomly at intervals of 15 minutes with a variation range of ±0.05 p.u. [86] and ±0.02 Hz, respectively. Two cases are considered : In the first case, the variations of ambient temperature, voltage and frequency are all taken into account, while they are neglected in the second case. Simulation results are shown in Figure 3.6 which shows that the active power profile strongly depends on the variations of ambient temperature, voltage and frequency, and hence these factors should be taken into account when estimating the power consumption of a TCL population.
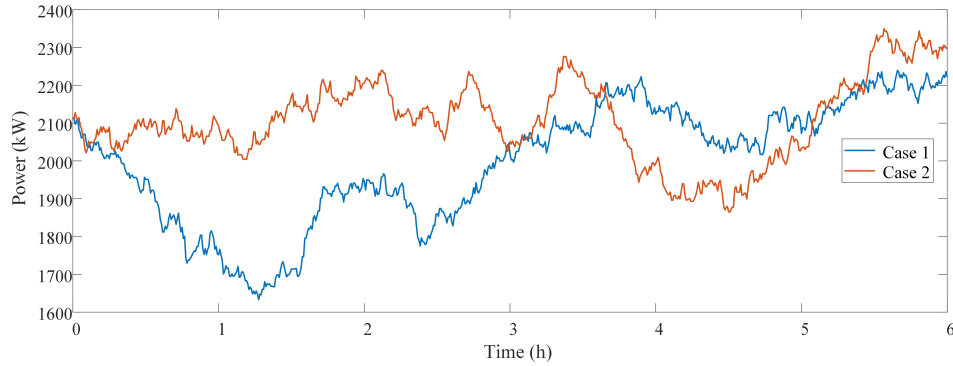
Figure 3.6 Combined effect of ambient temperature, voltage and frequency on the power profile of a TCL population

3.2 State Bin Transition Model of a TCL population

In this work, the state-bin transition model will be used for modeling the dynamic behavior of a TCL population. It has been shown that this modeling approach is simple yet sufficiently accurate for describing as well as predicting the behavior of a group of TCLs. It also allows handling the heterogeneity and uncertainties of a TCL population. It is noted that the Markov chains are regarded as a powerful tool for dealing with stochastic processes. A

motivation for using Markov chains is that, based on the past observations, the evolution of the process over time can be described in a probabilistic manner assuming that the future system state does not depend on its preceding state. Details about the state-bin transition model will be provided in the following.

To efficiently describe the dynamics of a TCL population over time, the state-bin transition model previously proposed in [47–50] is adopted. As the proposed aggregation approach deals with a heterogeneous population with different parameters (set-temperature, thermal resistance, thermal capacitance, power consumption, etc), the first step in the aggregation method is to normalize the temperature using the following expression [65]:

$$T_n^k = \frac{T^k - \left(\frac{T_{set} - \delta_{db}}{2}\right)}{\delta_{db}} \tag{3.8}$$

where T and T_n are the temperature and normalized temperature, respectively. T_{set} is the temperature set-point and δ_{db} is the width of the temperature dead-band.

Then, the normalized temperature interval is divided into $\frac{N_b}{2}$ equal slots as shown in Figure 3.7 and each resulting slot is further split into an ON-state bin and OFF-state bin. In this way, bins ranging from 1 to $\frac{N_b}{2}$ correspond to TCLs in the ON-state while those from $\frac{N_b}{2} + 1$ to N_b represent TCLs in the OFF- state. Each TCL among the TCL population must be placed on one of the N_b bins. In this way, each state bin will contain a certain fraction of TCLs. To better understand this concept, we consider the example of a TCL in the ON-state with a temperature set-point , a deadband and actual temperature equal to 20°C, 2°C and 19.5°C, respectively. Based on the previously described process, this TCL will be placed in the 5th bin. As the actual temperature of the TCL will increase over time, its bin position will change. Therefore, in order to get a global idea on the collective behavior of TCLs, it would be desirable to track the evolution of the fraction of TCLs in each bin over time. This aggregated model will serve as a basis for estimating the available control reserves as will be detailed hereunder.

3.3 Available Control Reserve Estimation and Prediction

The available control reserves are the amount of power change that can be offered by a TCL population participating in the provision of ancillary services. Estimating and predicting these reserves is the key to participation in the energy market. This task is performed by an aggregator that acts as an intermediate agent between TCLs and the ancillary services market. In this subsection, the role of an aggregator and its responsibility of integrating

Feasible bounds

	OFF State	N_b	N_b-1	$\cdots$	N_{end}^{off}	$\cdots$	N_{sta}^{off}	$\cdots$	$\frac{N_b}{2}+2$	$\frac{N_b}{2}+1$
	ON State	1	2	$\cdots$	N_{sta}^{on}	$\cdots$	N_{end}^{on}	$\cdots$	$\frac{N_b}{2}-1$	$\frac{N_b}{2}$

0   Tn δ_{db}

→ Natural Transition
→ Controlled Transition
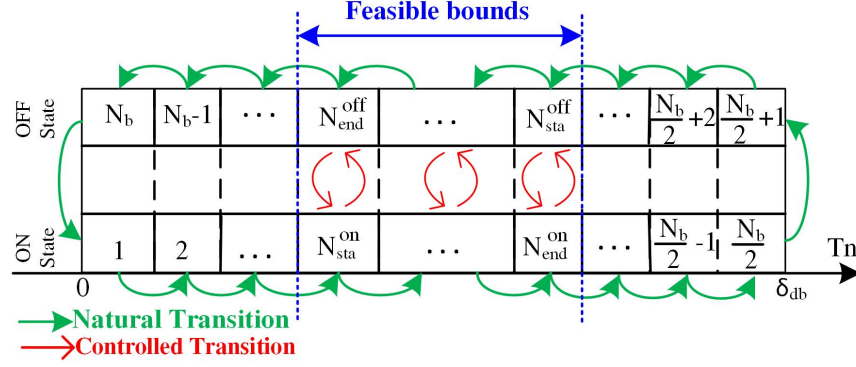
Figure 3.7 One-Dimension state bin transition model for a heating device and feasible bounds.

TCLs in the ancillary services market is introduced. The focus will be on presenting the approaches used for estimating the control reserves to be bid in the market. To this aim, two approaches, namely the classical Markov Chain approach and the supervised neural network-based approach will be presented.

3.3.1 Aggregator Role

As previously discussed, a single TCL with its limited capacity cannot participate individually in the ancillary services market because its power is well below the minimum amount of power required from each market participant. Therefore, an aggregator is needed to play the role of an intermediate entity between the market and a cluster of TCLs.

In general, the aggregator signs contracts with TCL owners that will allow him to manage their flexibility and trade it in the energy market. The aggregator will act as a TCL manager having 'contracting' or 'trading' role at the energy market side and a 'commanding' role at the TCLs side [67].

At the market side, upon the estimation of the available consumption flexibility of the TCLs, the aggregator bids this amount of power in the market as an 'energy offer curve' [87]. As the provided services are in the scale of seconds to a few minutes, bidding occurs at very short-term scales (e.g. 2 minutes, 5 minutes, etc) with high time resolution (order of seconds) [40]. Having done the clearing process at the ancillary services market level, the required amount of power is selected regarding other energy offers and is allocated to the aggregator. The aggregator is committed to delivering the contracted amount of power whenever needed otherwise penalties may be accorded. Similar to the conventional generators, the aggregator gets remuneration for the availability and the utilization of the contracted amount of reserve [88]. It is noted that contracts from bidding and clearing process are made continuously at very

short-term scales (e.g. 5 minutes in the PJM market) to meet the availability requirements of the primary and secondary control that operate at time scales in the order of seconds to a few minutes [89].

At the customer side, the aggregator is committed to coordinate the participation of all TCLs in the provision of ancillary services in a non-disruptive way i.e. the TCL temperature must always be kept within the permissible deadband to maintain the comfort. Furthermore, when selecting the set of controllable TCLs i.e. those that can participate in the control time interval, constraints such as the minimization of the number of switching and short-cycling should be taken into account to ensure a wide user acceptance [48].

To conclude, the aggregator needs to estimate the available flexibility that TCLs under its jurisdiction can offer in order to participate in the ancillary services market. This has to be done without compromising customers comfort while minimizing the wear and tear of the device. The aggregator needs, therefore, a mathematical tool for the accurate estimation of the available control reserves with lead times in the order of minutes and time resolutions in the order of seconds. In this report, two mathematical modeling approaches are utilized. The first approach is based on the Markov Chain model of the population which is already presented in various works such as [47–50]. The second approach is new and is based on using the supervised neural network.

A control period t_s (e.g. 5 minutes, 2 minutes, etc.) is considered assuming a prediction horizon p, for the aggregator. In general, to estimate the available control reserve of a TCL population, the first step is to select the controllable TCLs that are not supposed to switch their ON/OFF status during the upcoming time interval (i.e. during t_s). These TCLs can be controlled by the aggregator. The second step is to use a prediction model of the TCL population to estimate the available power during the control interval.

3.3.2   Reserve Estimation based on Hidden Markov Chain

Markov Chain process

The evolution of TCLs within the state-bin framework as described in the previous paragraph is perfectly a Markov Chain process. In general, a Markov chain is a mathematical way to describe a stochastic process. The principle of the Markov chain is as follows: If we consider a set of states $(S_1, \ldots, S_{N_b})$ as shown in Figure 3.8 then at any given state, the process can jump from its current state to another state. For example, considering that the chain is currently in the state S_i, then in the next timestep it can move to the state S_j with a probability p_{ij} as shown in Figure 3.8. These probabilities satisfy the condition $\sum_{1 \leq j \leq N_b} p_{ij} = 1$. An important

feature of the Markov chain process is that the behavior of the process in the next time step does not depend on the previous states taken by the chain before the current state S_i. A matrix called 'Markov Transition Matrix (MTM)' can be obtained to describe the probability of transition between states [90].
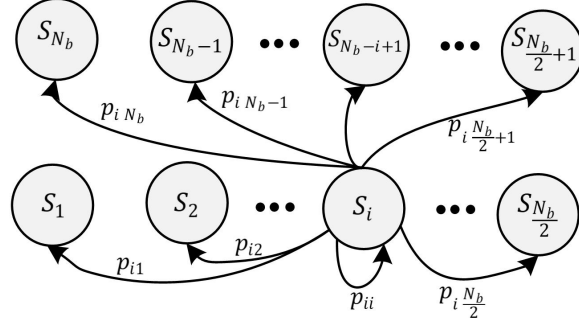
Figure 3.8 The Markov Chain process.

The description of the state bin framework previously presented is fully matched with the concept of Markov chain, provided that the states of the Markov chain $(S_1,\ldots,S_{N_b})$ are the state bins. In this case, describing the time-varying dynamic evolution of a population of TCLs comes to tracking their transition over time from one bin to another. In this way, the state-space model based on the MTM can be derived as follows:

$$x^{k+1} = Ax^k + Bu^k \tag{3.9}$$

$$y^k = Cx^k \tag{3.10}$$

Each element of the state vector x_i^k contains the fraction of TCLs in the ith state bin. Positive/Negative components of control vector u denote the fraction of TCLs to be switched ON/OFF. $A \in \mathbf{R}_{(N_b,N_b)}$ is the transpose of Markov transition matrix in which each element A_{ij} represents the probability of moving to the ith state bin provided that the process is currently in the jth state bin. Matrices $B \in \mathbf{R}_{(N_b, \frac{N_b}{2})}$ and $C \in \mathbf{R}_{(1,N_b)}$ are constants and and read [65],.

$$
B = \left[
\begin{array}{cc|cc}
1 & & & 0 \\
& \ddots & & \\
0 & & & 1 \\
\hline
0 & & & -1 \\
& \ddots & & \\
-1 & & & 0
\end{array}
\right]
$$

$$C = \bar{P} N \begin{bmatrix} 1, & \ldots & 1, & 0 & \ldots & 0 \end{bmatrix}$$

where N is the total number of TCLs and $\bar{P}$ is the average power consumption of TCLs.

Derivation of the A-matrix

As described earlier, the A-matrix contains estimates of the transition probability from one state bin to another. Each state bin can be defined uniquely by two states: the temperature and the switch status. In other words, if these two states are known for each TCL, it can be classified in the appropriate state bin. The states (temperature and switch status) of each TCL are assumed to be known through measurements done at regular control sampling times. Therefore, the hidden-Markov model parameter estimation from these measured states can be used for deriving the A-matrix. The Matlab function "hmmestimate" can be used to approximate the transition matrix based on the known sequence of previous states experienced by the model.

Practically, to reduce the amount of exchanged data, the collection of TCLs' states is preferred to be done at relatively long time intervals in the order of minutes rather than seconds. In this case, model equations (3.9)-(3.10) can be used to generate states (in the order of seconds) between two sampling times. This "collect-and-correct" procedure results in very reduced communication requirements and accurate temperature forecasts as has been proven in [66].

Selection of the controllable TCLs

The controllable TCLs are the TCLs that are unlikely to switch their status naturally from ON to OFF or from OFF to ON during the forthcoming control interval of length t_s. In this way, a controllable TCL will not switch its status unless it receives an external control signal (i.e any switching signal that is different from its thermostat control). The identification of controllable TCLs is therefore prediction-based, and it can be performed in a probabilistic way with recourse to the Markov Chain as suggested in [65]. This method relies on choosing the set of state bins called 'feasible bins' whose corresponding TCLs are unlikely to switch status. Details about the process of selecting controllable TCLs will be explained in the following.

The prediction horizon is defined as:

$$p = \frac{t_s}{t_m} \tag{3.11}$$

where p is the prediction horizon, t_s is the control interval, and t_m is the sampling interval.

Two functions are defined:

$$f_{off-on}(m,p) = \sum_{i=1}^{\frac{N_b}{2}} A_{(i,m)}^k \tag{3.12}$$

$$f_{on-off}(m,p) = \sum_{i=\frac{N_b}{2}+1}^{N_b} A_{(i,m)}^k \tag{3.13}$$

The function in (3.12) (resp.(3.13)) expresses the transition probability of the mth bin from OFF to ON status (resp. ON to OFF status) after p time steps where p is the prediction horizon defined in equation (3.11). An important aspect of A is that, estimating the transition probabilities in the next k time steps ($k \in [1,p]$) is equivalent to calculating $A^k = \left(A_{(i,j)_{1 \le i,j \le N}}^k \right)$.

Feasible bin intervals for ON and OFF devices are respectively $[N_{sta}^{on}, N_{end}^{on}]$ and $[N_{sta}^{off}, N_{end}^{off}]$ as shown in Figure 3.7, and are fixed in a way that functions (3.12) and (3.13) be smaller than the predefined thresholds α_{set} and β_{set}, respectively. In this work, α_{set} and β_{set} are both set to 10%. It is noted that when a TCL changes its switch status, it jumps from its current bin to the bin with the same temperature but with the opposite switch status.

In more details, the intervals $[N_{sta}^{on}, N_{end}^{on}]$ and $[N_{sta}^{off}, N_{end}^{off}]$ can be determined as follows:

- N_{end}^{on} (resp. N_{end}^{off}): As ON-TCLs (resp. OFF-TCLs) in state bins close to bin $\frac{N_b}{2}$ (resp. N_b) are near the edge, they are more likely to be switched OFF (resp. ON) by the internal thermostat-control described in equation (3.7). Thus, TCLs within $[N_{end}^{on}, \frac{N_b}{2}]$ (resp. $[N_{end}^{off}, N_b]$ will not be nominated to participate in the control process. ;

- N_{sta}^{on} (resp. N_{sta}^{off}): ON-TCLs close to bin 1 (resp. bin $\frac{N_b}{2}+1$) have just been switched from OFF to ON (resp. ON to OFF) a short time ago. Besides, if a TCL within the interval $[1, N_{sta}^{on}]$ (resp. $[\frac{N_b}{2}+1, N_{sta}^{off}]$) is chosen to participate in the control service, then it will move to the interval $[1+N_b-N_{sta}^{on}, 1]$ (resp. $[1+N_b-N_{sta}^{off}, \frac{N_b}{2}]$) in which it is more likely to switch to ON (resp. OFF) status again by the internal thermostat-control.

Accordingly, N_{end}^{on} , N_{end}^{off} , N_{sta}^{on} and N_{sta}^{off} can be calculated by:

$$\forall n \in [N_{end}^{on}, \frac{N_b}{2}] \quad f_{off-on}(n,p) > \alpha_{set} \tag{3.14}$$

$$\forall n \in [1, N_{end}^{on}] \quad f_{on-off}(n,p) \le \alpha_{set} \tag{3.15}$$

$$\forall n \in [\frac{N_b}{2}+1, N_{end}^{off}] \quad f_{off-on}(n,p) \le \beta_{set} \tag{3.16}$$

$$\forall n \in [N_{end}^{off}, N_b] \quad f_{off-on}(n, p) > \beta_{set} \tag{3.17}$$

$$N_{sta}^{on} = 1 + N_b - N_{end}^{off} \tag{3.18}$$

$$N_{sta}^{off} = 1 + N_b - N_{end}^{on} \tag{3.19}$$

where α_{set} and β_{set} are both set to 10%.

Estimation of the Available Control Reserves

The available active/reactive control reserve is the available active/reactive power offered by controllable TCLs within the feasible bin intervals for down- and up-control. It is noted that the up- and down-control reserves are used, respectively when a power reduction or a power increase is needed. Control reserves at time step k can therefore be estimated by [65]:

$$P_{max}^- = \sum_{i=N_{sta}^{on}}^{N_{end}^{on}} x(i).P_{sum} \tag{3.20}$$

$$P_{max}^+ = \sum_{i=N_{sta}^{off}}^{N_{end}^{off}} x(i).P_{sum} \tag{3.21}$$

where subscripts + and - refer to up and down control, respectively. P_{max}^- and P_{max}^+ are the available power for down and up control, respectively; $x \in \mathbf{R}_{(N_b,1)}$ is the state vector; P_{sum} is the total power consumption of all TCLs. At the beginning of the control interval, if we assume that the measurement of the state vector is available, then the vector x is considered equal to the measurement state vector x_{meas}. The estimation of the available power in each of the next k time step ($k \in [1, p]$) is based on equations (3.9)-(3.10). It is noted that the available reactive power Q_{max} for control can be deduced from the active power based on the power factor of the TCLs.

Model Performance

In this part, we aim to investigate the performance of the Markov Chain approach for predicting the available control reserves considering various factors including the number of state bins, the length of the prediction horizon, and the variations of the ambient temperature. In all cases, a population of 1500 TCLs with the parameters depicted in Table 3.1 is simulated during 6 hours. The simulation time step is set to 30 seconds and the state at the beginning of each control interval is supposed to be known from the measurement. The A-matrix is generated based on the preceding 400 states (Temperature and switch status) and updated

hourly. The indicator used for assessing the performance of the prediction model is the coefficient of variation (CV) defined as follows:

$$CV = 100 \times \frac{\sqrt{\frac{\sum_{i=1}^{n}(y_i - \hat{y}_i)^2}{N_{obs}}}}{\bar{y}} \tag{3.22}$$

where N_{obs} is the number of observations; y_i is the estimated aggregated power obtained with the Markov chain approach, $\hat{y}_i$ is the aggregated active power obtained from the individual TCL models, and $\bar{y}$ denotes the average active power.

Variation of the number of state bins: The aim of this part is to investigate the effect of the number of state bins on the model performance. The ambient temperature and the prediction horizon are set to 5°C and 2 minutes, respectively. Different numbers of state bins ranging from 10 to 120 are considered, and the calculated CV for each case is reported in Table 3.2. The comparison between the predicted power profiles and that obtained from the individual TCL model for a number of bins equal to 40 is illustrated in Figure 3.9.
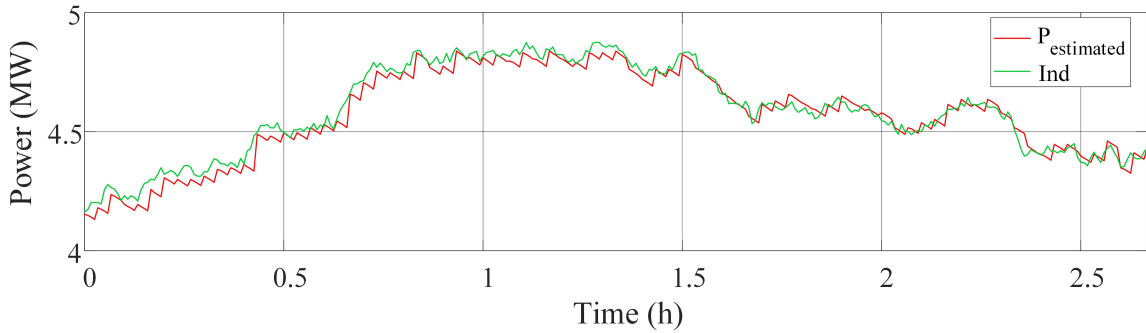
Figure 3.9 A comparison of TCLs' predicted aggregated power and individual TCL model.

The obtained CV for different values of state bins are overall indicating an accurate prediction as can be seen in Table 3.2 and Figure 3.9. However, it is clear that the relation between the number of state bins and the CV is not linear and the CV is not strongly affected by the number of state bins. The best performance is obtained with the state bin numbers ranging from 40 to 70. It is noted that a larger number of state bins implies the use of larger matrices. Therefore, as a compromise between accuracy and computational burden, the number of state bins adopted in this work is 40.

Variation of the prediction horizon: To investigate the effect of the length of the prediction horizon on the estimation accuracy, various prediction horizons ranging from 1 to

Table 3.2 Coefficient of variation obtained by the Markov Chain approach with different numbers of state bins

N_{bin}	10	20	40	60	70	80	100	120
CV(%)	0.9026	0.9147	0.8995	0.8684	0.8803	0.8840	0.8823	0.8683

5 minutes are considered. The ambient temperature and the number of state bins are set to 5°C and 40, respectively. The obtained values of CV are illustrated in Table 3.3 and the aggregated power profile calculated for each case is compared with the individual TCL model as shown in Figure 3.10.

Table 3.3 Coefficient of variation obtained by the Markov Chain approach with different prediction horizons

p	2 (1 min)	4 (2 min)	6 (3 min)	8 (4 min)	10 (5 min)	12 (6 min)	14 (7 min)
CV(%)	0.5993	0.8995	1.1927	1.5484	1.6911	2.0934	2.3855
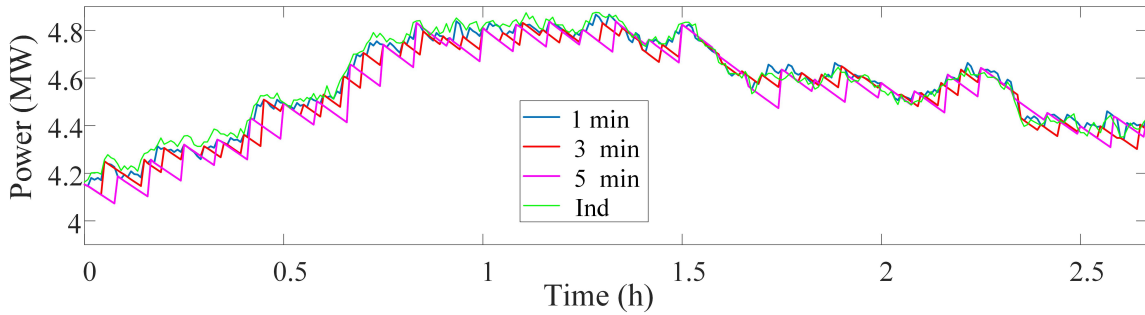
Figure 3.10 A comparison of TCLs aggregated power with different prediction horizons

The obtained results show that the smaller is the time step, the more accurate is the estimation. Moreover, large prediction horizon can result in lower prediction accuracy. As the prediction horizon determines the frequency of data exchange between the aggregator and both the market and the individual TCLs, it is preferred to have a relatively long control interval (i.e., large prediction horizon) to reduce the communication burden. A prediction horizon of 2 minutes seems to provide a reasonable trade-off between the estimation accuracy and the communication requirements which is the choice adopted in [65].

Variation of the ambient temperature, voltage and frequency: In this part, the performance of the Markov Chain approach is investigated under time variations of ambient temperatures, voltages and frequency. The ambient temperature variations are taken from

the weather station ISEP/IPP with a time resolution of 5 minutes. Voltage and frequency variations are generated randomly at intervals of 15 minutes with a variation range of ±0.05 p.u. and ±0.02 Hz, respectively. As different CVs are obtained depending on the random initial conditions and random TCLs' properties, 511 random experiments are conducted, and the obtained CVs are illustrated in Figure 3.11.
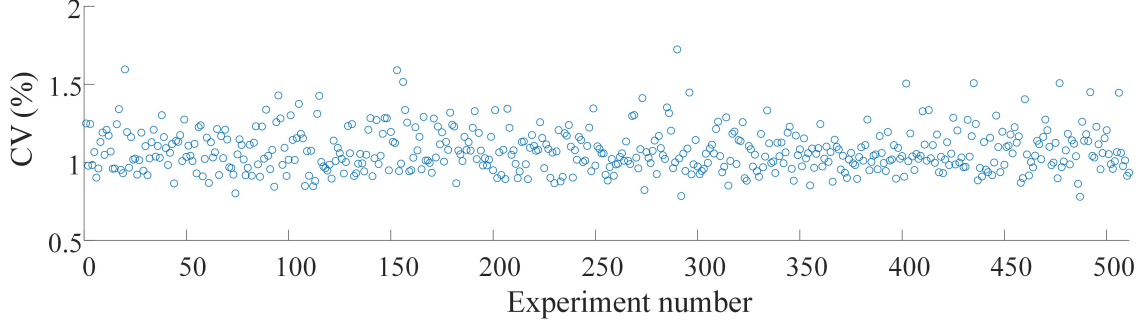
Figure 3.11 Performance of the Markov Chain based aggregated model under variations of ambient temperature, voltage and frequency

The obtained CV percentages are mainly concentrated in the interval [0.8, 1.2] which is an acceptable range. However, this performance is prone to some slight errors as compared to the case with constant ambient temperatures, voltage and frequency are assumed constant.

Issues with the A-matrix

As has been discussed in [65], the derivation of the A-matrix is performed offline based on the historical data about TCLs' states. However, the times at which the A-matrix should be updated has not been defined properly. For instance, in [65] and in our previous simulation results, the A-matrix has been updated hourly. In some studies such as [49] an analytical derivation of A-matrix is obtained and it has been shown that the A-matrix depends on the ambient temperature. It means that, whenever the ambient temperature varies, a new estimation of the A-matrix is required. As the ambient temperature fluctuates continuously, a possible solution is to continuously update the matrix very frequently. However, such a solution is not practical, especially in very small time-scale control applications such as frequency control. Another solution is to pre-define a set of matrices offline for different ambient temperatures, i.e. preparing a look-up table [48]. Although this solution allows avoiding the online computational burden, it implies extensive unnecessary computations. Furthermore, a common problem with these approaches is the lack of generality since the variations of the voltage and frequency are not taken into account for the A-matrix calculation. This explains the degraded behavior obtained in the previous simulation results when the ambient

temperature, frequency and voltage variations were added to the simulation. It is noted that obtaining an accurate analytical expression for the A-matrix is mathematically complex. In the following, we attempt to address the above-mentioned shortcomings by proposing a new tool for reserve estimation based on the neural-network approach.

3.3.3 Reserve Estimation based on Supervised Neural Networks

We propose a novel model based on a machine learning approach that allows estimating and predicting the available reserves provided by TCLs. The proposed model attempts to realize the same tasks of the Markov Chain approach in terms of selecting controllable TCLs and estimating the aggregated reserve, without the limitations of the Markov Chain model.

As has been discussed earlier in this report, the controllability and the aggregated power of a TCL population depends mainly on the ambient temperature, frequency and voltage. Since these data are readily available by measurements and can be collected offline, it would be of interest to express the available reserve of a TCL population as a function of these data.

Formulation of the Artificial Neural Network

The first step prior to creating a neural network is to define the inputs and outputs. Before defining the formulation of the neural network, a controllability indicator F is defined to identify the controllable TCLs. $F \in \mathbf{R}_{(N_b,1)}$ is a vector whose each component F_i holds the percentage of the TCLs initially in state bin i move to opposite state bins after p time steps where p is the prediction horizon. For example, if N_b is equal to 40, F_{10} contains the percentage of TCLs currently in the 10th bin that will move to the opposite bins that are the bins ranging from $\frac{N_b}{2} + 1$ to N_b after p time steps. The feasible bins are those having a controllability indicator of less than 10%.

The structure of the proposed neural network is shown in Figure 3.12 where three output vectors are considered:

- $(P_{max,i})_{1 \leq i \leq p}$ represents the control reserve (i.e. the available power for control) in the forthcoming control interval which has a size equal to the prediction horizon p.

- $(P_{agg,i})_{1 \leq i \leq p}$ represents the total power consumption of all TCLs in the forthcoming control interval which has a size equal to the prediction horizon p.

- $(F_i)_{1 \leq i \leq N_b}$ is the previously defined controllability indicator.
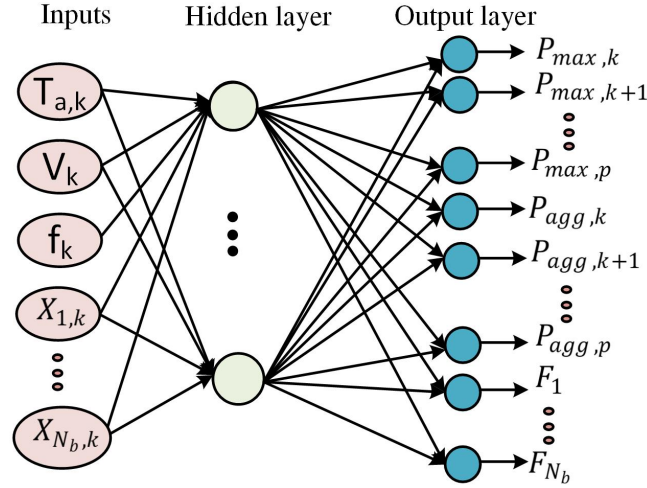
Figure 3.12 The proposed neural network structure

It has been shown previously that external parameters, namely ambient temperature, voltage and frequency affect the collective power consumption of TCLs. Moreover, the state bin information at the beginning of the control interval has an effect on future power consumption. Therefore, four input vectors are considered. The first three inputs are scalar, and they represent the ambient temperature, the voltage and the frequency at the beginning of the control interval. The fourth input is the state bin vector of size $N_b \times 1$.

The neural network is trained based on the 4-hour data where 70%, 15% and 15% of the data are used for training, validation and testing, respectively. The data are obtained based on the temperature variations that are taken from the weather station ISEP/IPP with reference to a real measurement site with a resolution of 5 minutes [85]. The voltage and frequency variations are generated randomly at intervals of 15 minutes with a variation range of $\pm$ 0.05 p.u. and 0.02 Hz, respectively. Outputs (targets) are obtained based on the individual TCL models. Sigmoid and linear transfer functions are used in the hidden and output neurons. The Levenberg-Marquardt back-propagation is used for training because of its robustness. Different hidden layer sizes are used and we found that the best result is obtained with 15 neurons.

It is noted that a primary advantage of the neural network over the Markov Chain is that it is trained only once unlike the MTM matrix that should be updated over regular time intervals (e.g. each hour). In fact, the A matrix is updated at each hour mainly because of the variable ambient temperature and the variable voltages and frequency. However, if we consider this information as an input to the neural network, then there is no need to train

a new network at each hour. It is trained only once and can be used at any time provided that the current ambient temperatures, voltage and frequency are delivered.

Model performance

In this part, the performance of the Neural Network approach is investigated and compared with the Markov Chain approach considering various factors, namely the length of the prediction horizon as well as variations of the ambient temperature, voltage and frequency. To be able to compare the performance of the Neural Network and the Markov Chain for each case, the same population of TCLs used in the Markov Chain model is used for testing the Neural Network. However, unlike the Markov Chain, the Neural Network is trained only once by use of the first 400 input-output data out of 6-hour simulation data (720 points).

Variation of the Prediction Horizon: The same conditions used in the case of the Markov Chain are used to evaluate the effect of the prediction horizon on the Neural Network performance. The resulting CV percentages are illustrated in Table 3.13. A comparison between the aggregated power profile obtained with a prediction horizon of 10 (i.e. 5 minutes) and that of the individual TCL model is shown in Figure 3.13.

Table 3.4 Coefficient of variation obtained by the Neural Network with different prediction horizons

p	2 (1 min)	4 (2 min)	6 (3 min)	8 (4 min)	10 (5 min)	12 (6 min)	14 (7 min)
CV(%)	0.6041	0.5818	0.6561	0.5367	0.6581	0.6679	0.6116
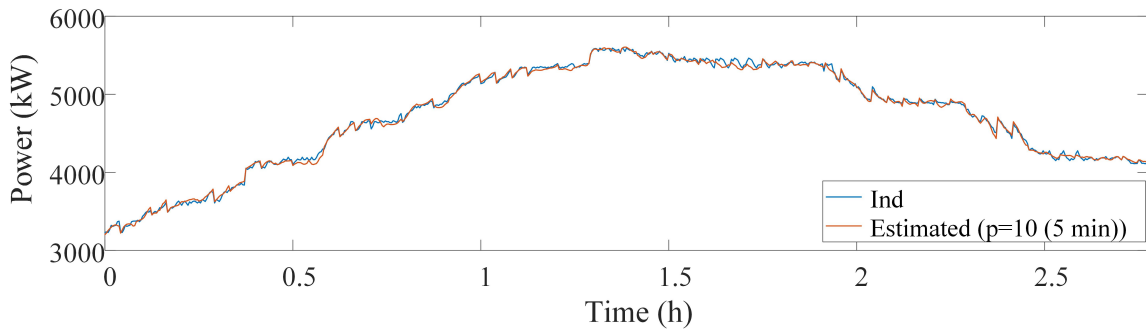
Figure 3.13 TCLs aggregated power obtained by the neural network with a prediction horizon of 10 time steps.

The CV values obtained with the neural networks and illustrated in Table 3.13 show a very good performance as it is not affected by the length of the prediction horizon unlike the

results obtained by the Markov Chain. It is seen from this figure that unlike the Markov Chain, the prediction accuracy is maintained for the long prediction horizons. Comparing Figure 3.13 and Figure 3.3, one can conclude that for a given prediction horizon, the neural network estimation accuracy outperforms the Markov Chain approach.

It is noted that with a number of bins N_b equal to 40, the feasible range of bins of ON and OFF state obtained by the neural network are [2, 19] and [22, 39] which is exactly similar to that of the Markov Chain approach.

Variation of the ambient temperature, voltage and frequency: The performance of the neural network approach under variations of ambient temperature, voltage and frequency is evaluated. We use the same 511 experiments previously employed for testing the Markov Chain. The CVs obtained with 511 experiments using both approaches are illustrated in Figure 3.14.
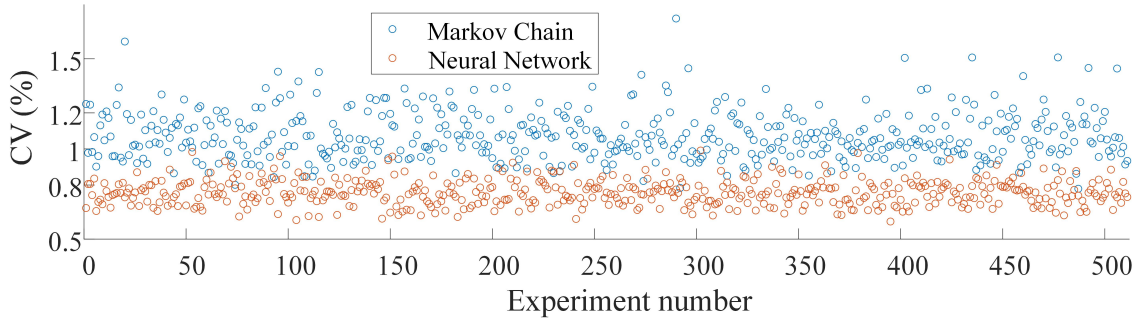
Figure 3.14 comparison of the performance of the Neural network and the Markov Chain approaches under variations of ambient temperature, voltage and frequency.

It can be seen from this figure that the neural network approach outperforms the Markov Chain in terms of prediction accuracy. The CVs obtained by the neural network take values within the interval [0.6, 0.8] while those obtained with the Markov chain are within the interval [1, 1.2].

One important consideration about the neural network, in general, is that its performance depends on the input data. Hence, the inputs should contain enough/sufficient information so that the input-output relations can be captured accurately.

3.4 Conclusion

In this Chapter, the individual TCL model has been presented and evaluated taking into account variations of the ambient temperature, the voltage and the frequency. It has been

shown through various simulations that the dynamic behavior of a TCL cluster strongly depends on the ambient temperature, frequency and voltage variations. Therefore such parameters should be taken into account when developing an aggregated TCL model. A neural network-based approach has been developed to estimate and predict the available control reserves offered by TCLs and has been compared with the classical Markov Chain approach. It has been concluded that the neural network approach outperforms the Markov Chain in terms of prediction accuracy. In contrast with the Markov Chain approach whose accuracy is significantly affected by the selected prediction horizon, the Neural Network approach remains accurate even for longer prediction horizons. In cases of varying temperature, voltage and frequency, although the neural network is not updated (trained only once), it showed a very good performance with very low CVs. The Markov Chain, however, provides less accurate estimation despite its hourly-based update.

CHAPTER 4   TCL MANAGEMENT FOR PROVISION OF PRIMARY AND SECONDARY CONTROL RESERVE

The estimation and prediction of the available control reserves were introduced in Chapter 3 using two different approaches that are the Markov Chain and the neural network-based approach. In this chapter, the estimated control reserves serve as a basis for managing a TCL population as a primary and secondary control reserve. In particular, the control parameters transmitted from the aggregator to TCLs are presented and calculated based on the available control reserves. Control methods for the provision of primary and secondary control by a TCL population are also described in detail in this Chapter.

4.1   Management of a TCL population by the aggregator

The aggregator manages the participation of TCLs in the energy market. The communication between the aggregator and the TCLs under its jurisdiction is enabled through a two-way communication. Each TCL is equipped with a local controller that allows it to exchange signals with the aggregator and at the same time decide on the switch-status of the TCL. TCLs are divided into two categories: TCLs that will participate in the primary and secondary control are referred to as TCLs in primary control mode (PCM) and TCLs in secondary control mode (SCM), respectively. The aggregator bids the estimated primary and secondary control reserves in the energy market. After bidding and clearing, amounts of cleared reserves are determined. The aggregator should, therefore, optimally coordinate the participation of TCLs under its jurisdiction based on the required amounts of active or reactive power. The aggregator appropriately manages the TCLs in order to have an aggregated response that respects the requirements of the delivered service that can be primary or secondary control. Furthermore, at the customer side, the comfort must be maintained by keeping the temperature within the deadband, and the device's wear and tear should be considered.

In this work, TCLs in PCM participate only in primary frequency control. Primary frequency control is the most challenging service as it requires an instantaneous response in order to stabilize the system in case of large deviations. Therefore, TCLs' response to any deviation must be instantaneous without compromising the customer comfort, while the number of switching per device is minimized. The short-cycling, which is the repetitive switching within a very short time period should be also minimized as it wears out the device. A suitable architecture to achieve these goals is the semi-autonomous control as it allows to optimize the

collective TCLs' response locally and at the global system level as it benefits from both the centralized and decentralized approaches. In fact, the decentralized approaches are mainly used in the primary control as they guarantee an instantaneous response while achieving local objectives such as maintaining the temperature within admissible ranges. However, it has been shown that these approaches lack a higher coordinating control level and may result in either over or under-response which makes it difficult to reach a system-level set-point. One can think of the centralized approaches to achieve an accurate system-level response. However, these approaches are rarely employed in the primary control due to their slow response to frequency deviations. In a semi-autonomous control scheme, the aggregator sends control parameters at regular control time intervals. These parameters instruct TCLs on how to behave within the control interval whenever a deviation occurs. It is noted that the control parameters are sent over relatively long time-intervals in the order of minutes while TCLs' response is instantaneous which guarantees a fast response and a low communication burden. These control parameters (e.g. trigger frequencies) are not direct control decisions but rather represent instructions that guide the local controller of the TCL in the choice of its control decisions. As the aggregator is regarded as a central unit that oversees the TCLs, the control parameters are chosen in a way to reach an appropriate system-level response that imitates the droop-based response of conventional generators. In this work, the semi-autonomous TCLs' operation is chosen for the primary frequency control.

As the secondary control is less demnanding than the primary control in terms of response speed, it can be performed in a centralized way to achieve an accurate system-level response, especially when resources other than TCLs are involved. In this case, TCLs response is not instantaneous but rather depends on the reception of direct switching signals from the aggregator. TCLs in SCM are assumed to have active and reactive power consumption so that they can have an effect on both active and reactive power flows. Therefore, those TCLs participate in the combined frequency and voltage correction. In this work, a centralized secondary control scheme is adopted.

In order to have a two-way communication with the aggregator, each TCL is equipped with a local controller. The local controller relies on a control algorithm that allows TCLs to react appropriately based on its mode that can be PCM or SCM. Moreover, the TCL local controller can measure frequency with a resolution of few mHz.

In this chapter details about the communication links (i.e. the exchanged data) between the aggregator and TCLs are provided. Control parameters are then defined in order to achieve the following objectives:

- In case of primary control, the reaction of TCLs to frequency deviations is instantaneous

and coordinated in a way to achieve an aggregated response similar to that provided by conventional generators.

- In case of secondary control, TCLs respond only upon the reception of switching signals from the aggregator.

- Short cycling is minimized by dividing TCLs into groups.

- The number of switching events is minimized by a proper ordering of TCLs.

4.2 Group division and prioritization

The first step in managing a TCL population introduced in Chapter 3 is the selection of controllable TCLs. Based on the measured temperature and switch status at the beginning of the control interval, the controllable TCLs are identified, which are those that are unlikely to naturally change their status during the control interval. A rank is then allocated to each TCL to prioritize its participation over other TCLs. To this aim, a rank $K_{rank,i}$ resulting from a merit order process is assigned to each TCL 'i'. It has been shown in various works such as [65, 68] that a convenient ranking criterion in order to minimize the number of switching events per TCL, is the temperature of the TCL. In this way, devices in ON-state with higher temperature are given top-priority as they are likely to spend a longer time in the OFF-state whenever they are required to switch status from ON to OFF. Similarly, devices in OFF-state with higher temperature are given top-priority as they are likely to spend a longer time in the ON-state whenever they are required to switch status from OFF to ON.

The controllable TCLs are then divided into groups in order to minimize short-cycling i.e. the repetitive switching of a device within a very short period of time. In fact, as the provided ancillary services are very fast (in the scale of seconds), a case of two or more successive deviations within a short period of time is very common which is harmful to the devices.

Dividing TCLs into groups is a solution to short-cycling as presented in [65]. The idea behind the grouping concept is that TCLs will take turns in responding to deviations. For example, if we consider two successive deviations and two TCL groups, then the first group responds to the first deviation while the second group responds to the second deviation. In this way, we avoid the case in which only one group responds to both deviations. The TCLs in ON-state are divided into N_{ON} groups while those in OFF-state are divided into N_{OFF} groups. The number of ON/OFF-groups is decided based on the available control reserves as follows:

$$N_{on} = \lfloor \frac{P_{max}^-}{P_{res}^-} \rfloor \; ; \; N_{off} = \lfloor \frac{P_{max}^+}{P_{res}^+} \rfloor \qquad (4.1)$$

with

$$P_{res} = \begin{cases} P_{prim} & in \quad Primary\ control\ mode \\ P_{TCL}^C & in \quad Secondary\ control\ mode \end{cases} \tag{4.2}$$

where N_{on} and N_{off} are number of ON and OFF groups, respectively, superscripts '+' and '-' denote up or down control, respectively. P_{max} is the available control reserve estimated by the aggregator, P_{prim} is the amount of the primary reserve calculated from the market clearing process; P_{TCL}^C is the amount of power requested from the aggregator for the secondary control, with P_{TCL}^C being less or equal to the amount of the cleared secondary reserve P_{sec}. It is noted that up control (resp. down control) refers to the case in which a power reduction (resp. increase) is required.

To better understand the concept, we suppose that at a certain time, the estimated available primary and secondary control reserves P_{prim} and P_{sec} are both equal to 2 MW. It is also assumed that control reserves are symmetrical i.e. up and down control reserves are equal. We assume that the cleared primary and secondary control reserves are set to 1 MW and that an energy management system (EMS) requests a power reduction P_{TCL}^C equal to 0.5 MW from the aggregator to be used in the secondary control. In this situation, the number of ON-groups and OFF-groups are 2 and 4, respectively.

Group indices indicating the group affiliation of each TCL'i' are calculated as follows:

$$G_{ind,i} = \left\lfloor \left| \frac{\sum_{k=1}^{K_{rank,i}} P_k}{P_{res}} \right| \right\rfloor \tag{4.3}$$

4.3   TCLs provision of primary frequency control

To realize the primary control, once a fast deviation event occurs, TCLs in PCM must react instantaneously with no communication based on local frequency measurements. Moreover, the aggregated response of the TCL population should mimic the classical generators in their way of responding to frequency deviations. In other words, from a higher-level viewpoint, the aggregation of TCLs should be viewed as a virtual generator acting based on its droop characteristic. Based on the cleared control reserves, the collective behavior should be similar to the droop curve presented in Figure 4.1 [66, 91]. The droop parameters are set to $\Delta f_{db} = 0.02Hz$ and $\Delta f_{max} = 0.2Hz$, which comply with the ENTSO-E requirements.

Droop coefficients for up and down control (K^+, K^-) can be determined based on Figure. 4.1 as follows:

$$K^+ = \frac{P_{prim}^+}{(f_0 - \Delta f_{db}) - (f_0 - \Delta f_{max})} \tag{4.4}$$
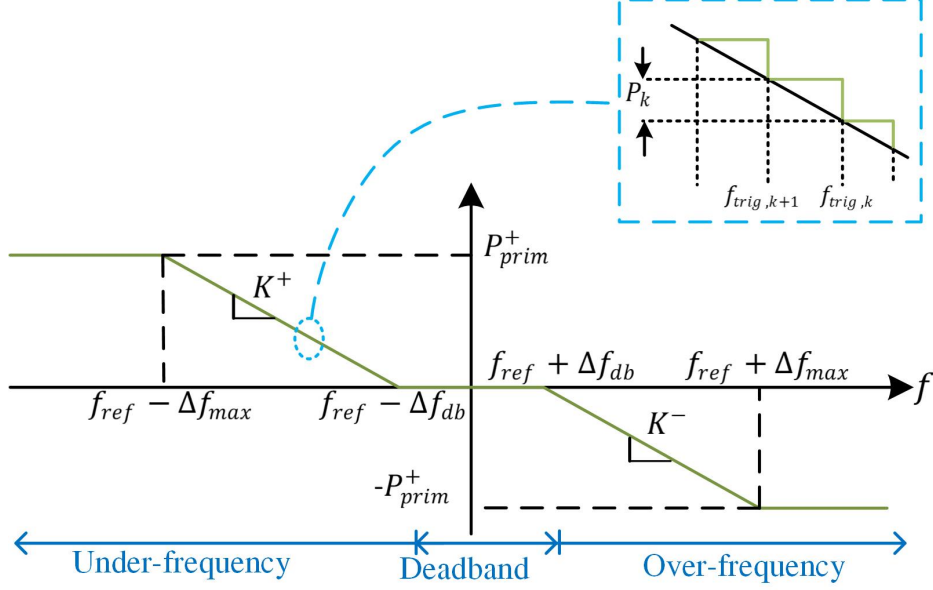
Figure 4.1 Aggregated frequency response of a TCL population

$$K^- = \frac{P^-_{prim}}{(f_0 + \Delta f_{max}) - (f_0 + \Delta f_{db})} \tag{4.5}$$

Such a droop-based behavior can be obtained by assigning an appropriate trigger frequency for each TCL at each control time interval of length t_s. Whenever the measured frequency exceeds or falls below the trigger frequency, appropriate action is taken by the local controller. For example, in the case of an under-frequency, if a TCL has a trigger-frequency f_i when the detected frequency falls below f_i, the device is turned off.

A proper definition of the trigger frequency assigned to each TCL allows having an aggregated response similar to a conventional generator. To this aim, each controllable TCL 'i' receives its own trigger frequency that allows it to react autonomously whenever a deviation event occurs based on local comparison of the actual frequency and the pre-defined trigger frequency. These trigger frequencies are defined as follows [65]:

- ON appliances:

$$f^-_{trig,i} = f_{ref} - \Delta f_{db} - q_i(f_{ref} - \Delta f_{db} - f_{min}) \tag{4.6}$$

$$f^+_{trig,i} = 2f_{ref} - f^-_{trig,i} \tag{4.7}$$

- OFF appliances:

$$f^+_{trig,i} = f_{ref} + \Delta f_{db} + q_i(f_{max} - f_{ref} - \Delta f_{db}) \tag{4.8}$$

$$f_{trig,i}^- = 2f_{ref} - f_{trig,i}^+ \tag{4.9}$$

with

$$q_i = \frac{\sum_{k=1}^{K_{rank,i}} P_k}{P_{res}} - G_{ind,i} \tag{4.10}$$

Therefore, to manage a population of TCLs as a primary reserve, the data to be exchanged between each TCL and the aggregator are the number of ON/OFF groups, the group index and the trigger frequencies. These control parameters are only sent at the beginning of the control time interval that is relatively long. The aggregator in return receives the temperature and switch status (ON/OFF) of the TCL periodically at the beginning of the control time interval. An illustration of the exchanged data among the aggregator and the TCLs in the PCM is shown in Figure 4.2.
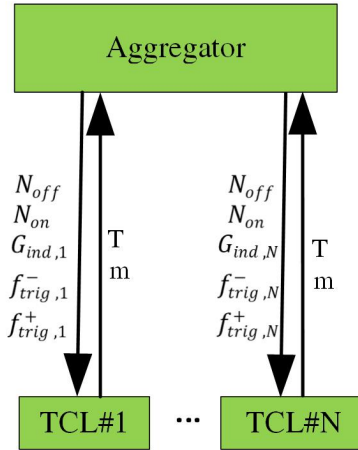
Figure 4.2 Data exchanged among an aggregator and the TCLs in PCM.

4.4 TCLs provision of secondary control

The secondary control aims to restore frequency and voltage to their permissible ranges. There exist usually different resources to participate in this type of control such as conventional generators, energy storage systems (ESSs), aggregations of electric vehicles, aggregations of TCLs, etc. As the secondary control is performed in a centralized manner, a central unit that oversees the different available resources optimally assigns new set-points for these resources or asks for specific power change (decrease/increase) amounts in case of loads. Therefore, to participate in the secondary control, the aggregator is requested to reduce or increase the aggregated power of TCLs by a specific amount P_{TCL}^C. This requested amount is a value within the intervals $[0 , P_{sec}^+]$ or $[-P_{sec}^- , 0]$ respectively in the cases of up and down regulation. Similar to the case of primary control, TCLs are divided into groups with equal

control reserve amounts. As the active and reactive power of TCLs are linked, any change in the active power consumption would induce a change in the reactive power as well. An illustration of the exchanged data among the aggregator and the TCLs in the PCM is shown in Figure 4.3.
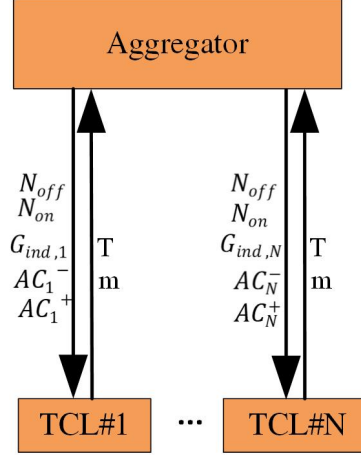
Figure 4.3 Data exchanged among an aggregator and the TCLs in SCM.

Based on the requested amount of power change, each aggregator decides about the TCLs that are to be used for the provision of the requested power; among the TCLs sorted in the merit-order list, the aggregator chooses those TCLs which can provide approximately the required power sum for regulation. For example, in the case of up control, the ranked TCLs are gradually switched OFF until the amount of power requested by the central controller is reached. Generally, switching signals are sent to TCLs from rank 1 to K_{rank} that satisfies:

$$P_{TCL}^C \cong \sum_{i=1}^{K_{rank}} P_i \tag{4.11}$$

To visualize the aggregated response of TCLs after reception of a control signal from an aggregator, a population of 500 TCLs with parameters shown in Table 3.1 is considered with the ambient temeperature of 5°C. The total simulation time is 30 min, and at t=8 min a control signal is sent to 50% of the TCLs in ON-state. The aggregated response of the population is illustrated in Figure 4.4. As can be seen in this figure, the aggregated power consumption of the population is reduced by almost the half and the reduction is maintained for a sufficient time (around 20 min) to perform the secondary control. It is noted that the secondary control is applied during around 15 minutes following the deviation.
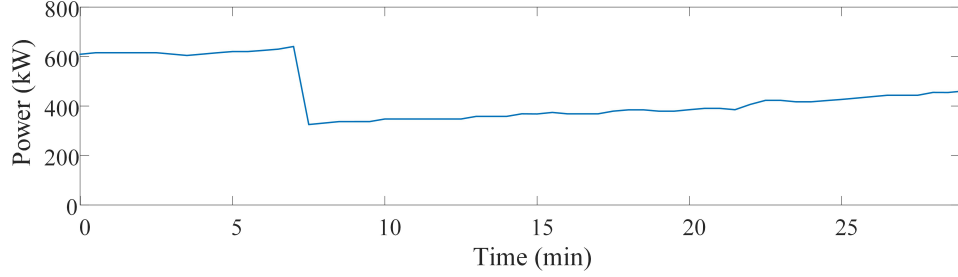
Figure 4.4 Aggregated power of a TCL population in response to direct switching signals.

4.5   TCL Local Controller

Each TCL is equipped with a local controller to enable two-way communication with the aggregator and to determine the device's switch status accordingly. At the beginning of the control interval of length t_s, each local controller sends the temperature and switch status of the TCL and receives control parameters from the aggregator. An illustration of the algorithm governing the operation of the local controller is shown in Figure 4.5.

To avoid conflicts between control reserves, it is assumed that a TCL can operate either in PCM or SCM (see block 'B1'), and it is the aggregator that decides on the operation mode. It is assumed that the operation mode is pre-determined in a day-ahead phase with a one-hour time window to reach an agreement among all actors [92], but this allocation is beyond the scope of this work. Thus, at the beginning of each hour, the aggregator updates the operation mode of the TCLs under its jurisdiction that can be PCM or SCM mode. It is noted that in the case of primary control, the local controller continuously measures frequency with an appropriate resolution.

The local controller algorithm ensures that the thermostat-control always has the highest priority (block 'B1') and that TCLs response to input signals depends on group affiliation to prevent short-cycling (blocks 'B4' and 'B5'). Furthermore, an autonomous operation is assured in case of PCM mode based on local frequency measurements. In the case of SCM an activation signal equal to "1" is received by the local controller when corresponding TCL is selected to switch status and set to "-1" otherwise (blocks 'B2' and 'B3').

4.6   Case study

The performance of the proposed control strategy for the primary frequency control is evaluated. The aim is twofold:

- (i) To see if the TCLs aggregated response replicates the behaviour of the conventional

$$If \quad T(t) \in [T_{set} - \tfrac{\delta_{db}}{2}, \ T_{set} + \tfrac{\delta_{db}}{2}]$$

B2
$$\begin{cases} If \ mode = "PCM" \\ \qquad SLC^+(t) = f_{meas}(t) - f_{trig}^+ \\ \qquad SLC^-(t) = f_{meas}(t) - f_{trig}^- \\ else \ if \ mode = "SCM" \\ \qquad SLC^+(t) = -AC^+ \\ \qquad SLC^-(t) = -AC^- \\ end \end{cases}$$

B3
$$\begin{cases} If \ [SLC^+(t) > 0 \ \& \ (SLC^+(t) \times SLC^+(t-\Delta t) \le 0) \ \& \ m(t-\Delta t) = 0] \\ || \ [SLC^-(t) > 0 \ \& \ (SLC^-(t) \times SLC^-(t-\Delta t) \le 0) \ \& \ m(t-\Delta t) = 0] \\ \qquad Ctr1(t) = 1 \\ \qquad S1(t) = 1 \\ else \ if \ [SLC^+(t) < 0 \ \& \ (SLC^+(t) \times SLC^+(t-\Delta t) \le 0) \ \& \ m(t-\Delta t) = 1] \\ || \ [SLC^-(t) < 0 \ \& \ (SLC^-(t) \times SLC^-(t-\Delta t) \le 0) \ \& \ m(t-\Delta t) = 1] \\ \qquad Ctr1(t) = -1 \\ \qquad S1(t) = 0 \\ else \\ \qquad Ctr1(t) = 0 \\ \qquad S1(t) = m(t-\Delta t) \\ end \end{cases}$$

B4
$$\begin{cases} If \ ctr1(t) \ne 0 \ \& \ ctr2(t-\Delta t) \ge 1 \qquad ctr2(t) = ctr2(t-\Delta t) - 1 \\ else \ if \quad ctr1(t) = 1 \ \& \ ctr2(t-\Delta t) = 0 \qquad ctr2(t) = N_{on} \\ else \ if \quad ctr1(t) = -1 \ \& \ ctr2(t-\Delta t) = 0 \qquad ctr2(t) = N_{off} \\ else \qquad\qquad\qquad\qquad\qquad\qquad\qquad\qquad ctr2(t) = ctr2(t-\Delta t) \\ end \end{cases}$$

B5
$$\begin{cases} If \ ctr2(t) = 0 \qquad m(t) = S1(t) \\ else \qquad\qquad\quad m(t) = m(t-\Delta t) \\ end \end{cases}$$

$$else \ m(t) = m_0(t) \ (thermostat \ control)$$
$$end$$

(**B1** encloses the full block)

Figure 4.5 TCL local controller algorithm

droop-based generators

- (ii) To investigate the coordination among the TCLs and the conventional generators.

To this aim, a dynamic simulation is performed using a conventional generator coordinated with a population of 500 TCLs with the parameters listed in Table 3.1. Each TCL is individually modeled by the algorithm of its local controller and, initially, 50% of the population is randomly distributed in the ON-state category.

A single-area power system is considered with the block diagram shown in Figure 4.6. The generators of this model are aggregated into an equivalent generator with a governor time constant TC_g and a turbine constant TC_t. The values used in this simulation, listed in Table 4.1, are taken from [66]. In this table, D and 2H are the load damping constant and

the inertia constant of the equivalent generator. The base power is 1000 kVA.
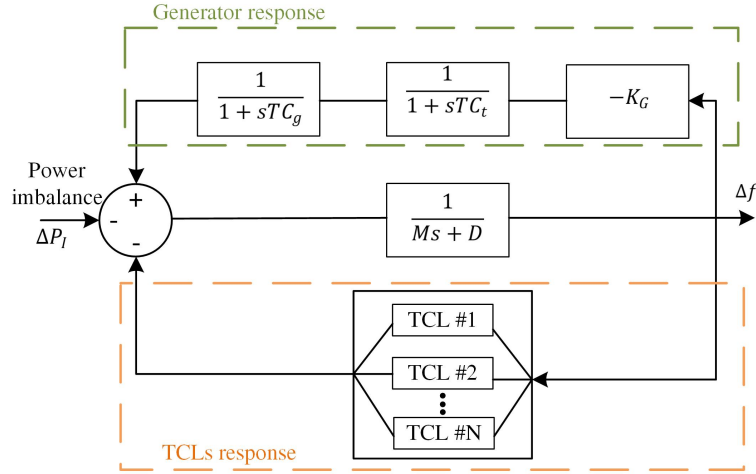
Figure 4.6 Block diagram of the studied simple single-area power system taken from [66].

Table 4.1 Simulation parameters [66].

Parameter	Value
TC_g	0.08 s
TC_t	0.4 s
D	0.015 p.u./Hz
M	0.1667

For the considered 500 TCLs, it is assumed that the amount of primary up and down control reserves are each equal to 450 kW in order to have a symmetrical reserve. The up/down droop coefficients (K^+,K^-) can be calculated accordingly. To have an equal active power sharing between the generator and the aggregation of TCLs, the value of the droop coefficient of the generator (K_G) is set equal to the droop coefficient of the TCL aggregation. Control parameters (trigger frequencies, number of ON/OFF groups, and group index) are calculated as described in Sections 4.2 and 4.3, and dispatched to the TCL controllers at the initial instant of the simulation.

Three cases are simulated:

- Sudden loss of 0.06 p.u. of generation

- Two successive sudden load change of 0.04 p.u. and 0.035 p.u.

- Participation of only TCLs in the frequency correction

The communication burden is then evaluated to highlight the advantage of the proposed control strategy over classical centralized control strategies.

4.6.1   Case 1: Sudden Loss of Generation

In this case, a sudden generation loss of 0.06 p.u. is simulated, and two scenarios are considered. In the first scenario, only the generator participates in the primary control while in the second scenario, both the generator and the TCL aggregation participate. Figure 4.7 shows the transient frequency response obtained only with the generator action compared with the frequency response obtained with the generator and TCLs combined control action. The share of the load mismatch between the aggregation of TCLs and the generator is shown in Figure 4.8.
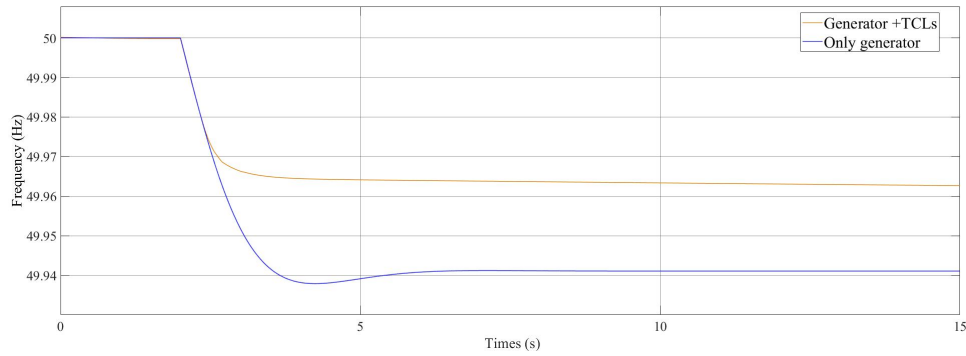
Figure 4.7 Frequency response subsequent to sudden generation loss of 0.06 p.u.. Case 1.
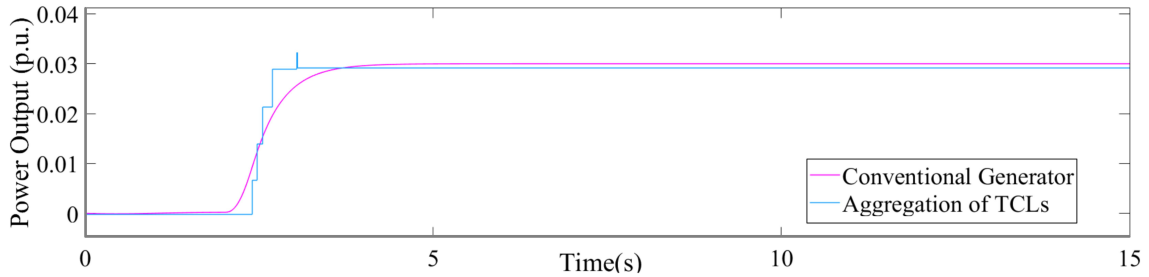
Figure 4.8 Output of the generator and TCL aggregation subsequent to sudden generation loss of 0.06 p.u.. Case 1.

Results show that the participation of TCLs in the primary frequency control improves the frequency response as the frequency nadir (lowest point of frequency) increases and the stabilization is faster compared with the case in which only conventional generator responds to the contingency event (see Figure 4.7). The aggregation of TCLs and the generator are equally sharing the load imbalance resulting from the generation loss as shown in Figure 4.8.

As expected, with 500 TCLs, the aggregated output power of the aggregation of TCLs is not perfectly smooth. This is due to the fact that TCLs cannot adjust their output power continuously and that the number of TCLs considered in the simulation is small. This has been already studied in [66] that has highlighted the difference between the real and ideal droop curves. Increasing the number of participating TCLs can make the load curve smoother and closer to the ideal one.

4.6.2 Case 2: Two Successive Load Change

The aim is to investigate the capability of a TCL-aggregation to respond to successive frequency deviations while illustrating the grouping concept. To this aim, two successive frequency deviations are simulated by a 0.04 p.u. and 0.035 p.u. load increase, respectively occurring at $t = 2s$ and $t = 10s$. An equal load mismatch sharing between the conventional generator and the aggregation of TCLs is assumed. The grouping procedure resulted in 2 ON groups and 3 OFF groups. In the category of initially-ON groups, there are two groups, $G1$ and $G2$, while in the category of the initially-OFF groups, there are three groups: $G1$, $G2$ and $G3$. The transient frequency response is shown in Figure 4.9. The changes in the aggregated power of the TCL population and the output power of the generator are shown in Figure 4.10 and Figure 4.11, respectively. The groups' activation in response to the successive deviations is illustrated in Figure 4.12.
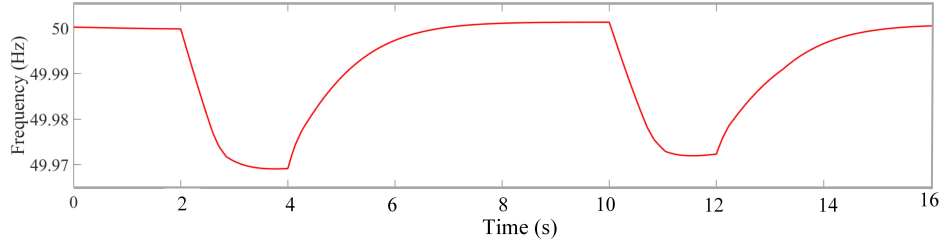
Figure 4.9 Frequency response subsequent to two sucessive sudden load change of 0.04 p.u. and 0.035 p.u.. Case 2.
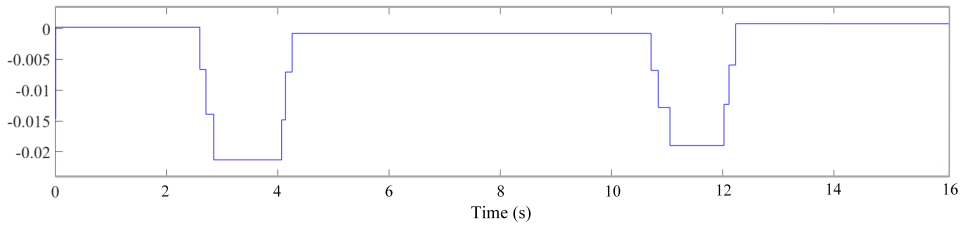
Figure 4.10 TCLs' aggregated power change subsequent to two sucessive sudden load change of 0.04 p.u. and 0.035 p.u.. Case 2.

It is seen that for both events, the coordinated action between the TCLs and the aggregator succeeds to bring back the frequency to the pre-defined frequency dead-band. In both events, the aggregator and the TCL aggregation equally share the load mismatch. It is noted that the TCLs start to react only when the frequency is outside the predefined dead-band as can be observed in Figure 4.10. Furthermore, as it is seen in Figure 4.12, in the category of initially-ON groups, while $G1$ responds to the first under-frequency event by switching its status, it is $G2$ that responds to the subsequent event which helps to avoid short-cycling. The TCLs in the group $G3$ do not change their status as there are only two deviations; hence, the participation of the group $G3$ is not needed. It is noted that initially-OFF groups $G1$ and $G2$ switch to a different state at the end of the first and the second frequency deviations respectively in order to restore the primary reserve and to be ready for the next contingency.
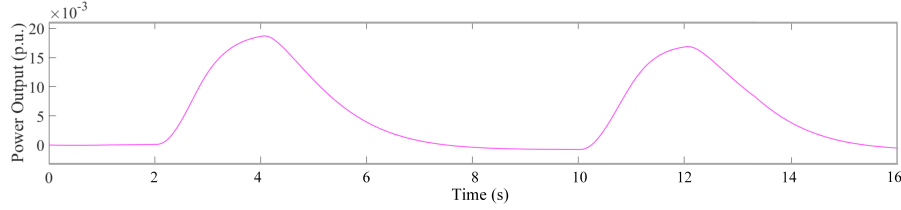
Figure 4.11 Generator output power change subsequent to two sucessive sudden load change of 0.04 p.u. and 0.035 p.u.. Case 2.
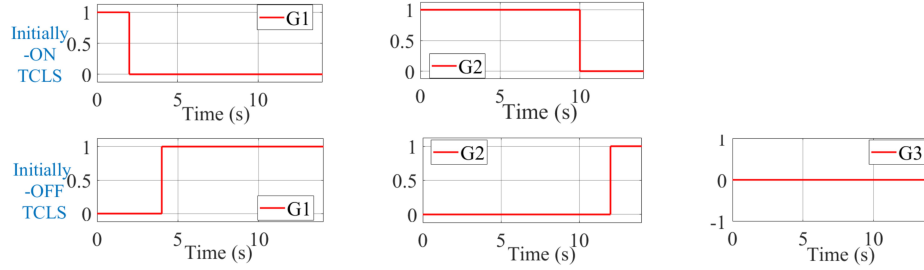
Figure 4.12 Groups activation subsequent to two sucessive sudden load change of 0.04 p.u. and 0.035 p.u.. Case 2.

4.6.3 Case 3: Participation of Only TCLs in the Frequency Correction

In this case, the capability of TCLs in responding to frequency deviations is tested during a 2-minute time interval. To this aim, the conventional generator action is disabled and only the TCLs respond to deviations. The load variations are simulated by Gaussian noise with a mean of 0 and a variance of 0.008. The system frequency with and without the action of

the primary control is shown in Figure 4.13. Results show that the frequency fluctuations are noticeably reduced by the action of TCLs.
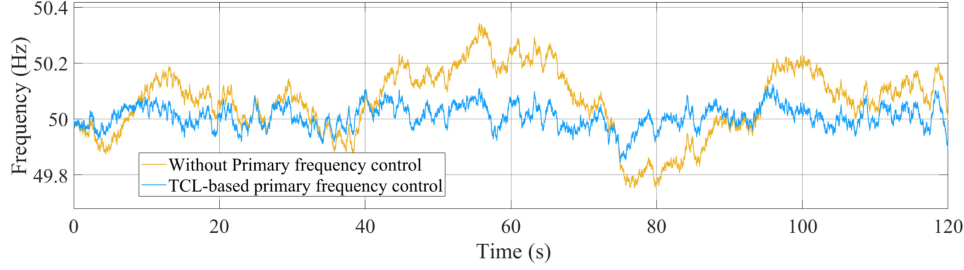
Figure 4.13 Frequency response with and without the primary control using only TCLs. Case 3.

4.6.4 Quantification of the communication needs

In this part, the communication needs of the proposed control strategy are compared with the conventional centralized control to highlight the efficiency of the semi-autonomous control method. The methodology employed in [66] is used to numerically quantify the communication needs.

Let D1, D2, D3, D4, D5 and D6 be:

- D1: The size of the temperature data

- D2: The size of the switch status (ON/OFF) data

- D3: The size of the direct switching signal

- D4: The size of the trigger frequencies data

- D5: The size of the number of ON/OFF groups

- D6: The size of the group index data

Let x_1, x_2, x_3, x_4, x_5 and x_6 be the number of times the previous data are sent to the local controller of the TCL during a time interval of 10 minutes. The number of the TCLs is denoted N and is set to 500. an indicator IND is used to determine the amount of data exchanged between the aggregator and a TCL, and it is defined as follows:

$$IND = N \times (x_1 \times D_1 + x_2 \times D_2 + x_3 \times D_3 + x_4 \times D_4 + x_5 \times D_5 + x_6 \times D_6) \qquad (4.12)$$

Centralized Control Strategy

In the classical centralized control strategy, the temperature and the switch status of the TCLs are collected every minute while direct switching signals are sent to each device at each second. This implies that: $x_1 = 10$, $x_2 = 10$, $x_3 = 60 \times 10 = 600$, $x_4 = x_5 = x_6 = 0$. Therefore:

$$IND_{conv} = 5000D_1 + 5000D_2 + 300000D_3 \tag{4.13}$$

Proposed control strategy

In the proposed control strategy, the temeperature and the switch status are collected every 2 minutes which implies that $x_1 = x_2 = 5$. There are no directly exchanged switching signals, therefore $x_3 = 0$. The trigger frequencies, the number of ON/OFF groups and the group indicators are sent every 2 minutes which implies that $x_4 = x_5 = x_6 = 5$. Therefore:

$$IND_{new} = 25000D_1 + 2500D_2 + 2500D_4 + 2500D_5 + 2500D_6 \tag{4.14}$$

It is assumed that:

- The size of a real number (D_1 and D_4) is two bytes

- The size of an integer (D_5 and D_6) is one bit

- The size of a binary variable (D_2 and D_3) is one bit

In this case, the calculated indicator for each case is as follows:

$$IND_{conv} = 315000 \; bit \tag{4.15}$$

$$IND_{new} = 15000 \; bit \tag{4.16}$$

This indicates that the communication needs of the proposed control strategy for the primary control are reduced by 95.24% compared with the centralized control strategy.

4.7   Conclusion

In this chapter, the control methods used by an aggregator for managing a TCL population as a primary and secondary control reserve have been proposed. Each TCL has a local controller to enable a two-way communication with the aggregator. The control signals

exchanged among the aggregator and TCLs have been presented. It has been shown through various simulation results that a proper definition of control parameters dispatched to TCLs allows to have an aggregated TCLs' response that imitates the behavior of conventional generators in primary and secondary control. Furthermore, TCLs participation does not compromise the customer comfort, while the number of switching events is minimized by a proper prioritization, and the short cycling is reduced by dividing the TCLs into groups. The particular focus has been given to the primary frequency control as it is the most challenging service, mainly in terms of response speed. The operation of TCLs in primary control is semi-autonomous in order to obtain a fast response with reduced communication burden. Moreover, is has been shown that the aggregated response of these TCLs emulates the droop-based behavior of conventional generators. Simulation results showed that the participation of TCLs in the primary frequency control significantly improves the transient frequency response.

CHAPTER 5   AN ENERGY MANAGEMENT SYSTEM FOR FREQUENCY AND VOLTAGE CONTROL OF MICROGRIDS

In this chapter, the control methods developed in Chapter 4 are incorporated into an energy management system (EMS) in which TCLs participate in the provision of the primary and secondary frequency and voltage control. First, The structure of the EMS is set forth with the relations between different actors. Aggregations of TCLs participate in both primary and secondary control. The secondary control is formulated as a PF-based multi-objective optimization. Finally, The effectiveness of the proposed control framework is tested on a typical MV microgrid for frequency and voltage control.

5.1   Proposed Energy Management System for Frequency and Voltage control

5.1.1   Hierarchical EMS structure

The proposed EMS is based on a hierarchical control framework, as shown in Figure 5.1. We consider a conventional microgrid comprising different DERs as well as controllable and non-controllable loads. DERs can include renewable distributed generators (such as photo-voltaic, wind turbine, etc.), dispatchable generators, and energy storage system (ESS). The main function of an EMS is to continuously balance generation and demand through the exploitation of available resources, i.e., dispatchable DGs, controllable loads, ESSs, and reactive power compensators (RPCs). A context of electricity-market full liberalization is assumed in which a market operator (MO) is responsible for managing a common AS market platform where available resources can bid their reserve offers [93].

5.1.2   Aggregator role

Aggregations of TCLs managed by an aggregator can be regarded as primary and secondary control reserves; hence, they can participate in the provision of frequency and voltage control. As has been discussed in the previous chapter, a proper definition of control parameters regularly dispatched to the TCLs from the aggregator makes their collective response similar to the behavior of conventional generators.

Actors participating in the control task send their bid offers to the ancillary service market including TCLs' aggregators. In fact, the aggregator estimates the available control reserve i.e. the available power that TCLs can offer for up or down control (P_{max}^+, P_{max}^-, respectively) using the neural network based aggregated model, and then sends the bid offer to the ancillary
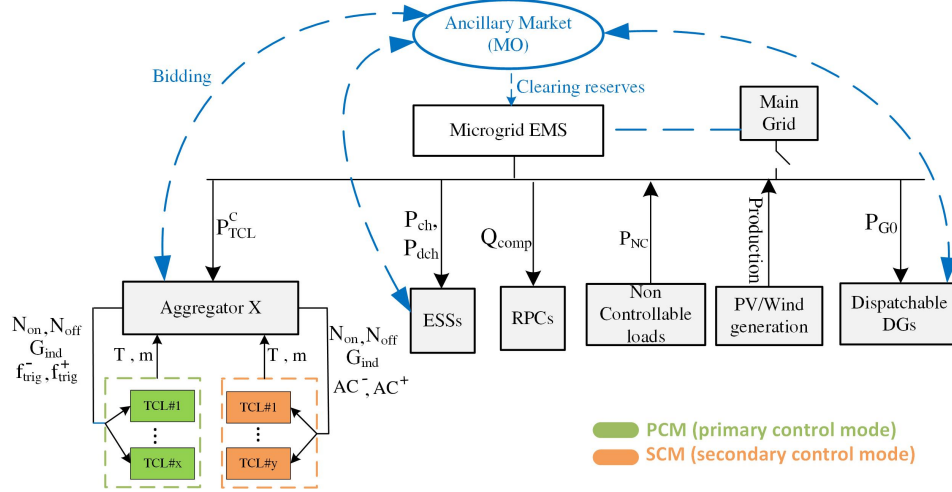
Figure 5.1 Proposed hierarchical EMS.

services market. Through the market clearing process, different offers of different resources compete against each other, and consequently, the cleared amount of power for primary and/or secondary control is dispatched to the aggregator and the EMS. The aggregator then coordinates the participation of the TCLs under its jurisdiction based on the requested amounts of power for primary or secondary control.

5.1.3   Control startegy

Grid resources that are reserved for the primary control must react instantaneously with no communication upon detection of a frequency deviation. The primary reserves are released based on the droop characteristics of the available resources including aggregations of TCLs. As has been discussed in Chapter 4, the control parameters dispatched to TCLs are the number of ON/OFF groups (N_{on},N_{off}), group index ($Gind$), trigger frequencies for up and down control (f_{trig}^+, f_{trig}^-), that are sent periodically at the beginning of the control interval of length t_s. The control interval is set to 2 minutes, which is relatively long to reduce the communication burden.

With particular reference to the Microgrid shown in Figure 5.1, the secondary control adopted in this work is centralized and relies on a PF-based multi-objective optimization taking in consideration microgrid topology, DGs' capacities and loads with the objective to simultane-ously minimize the voltage/frequency deviations as well as the grid operation cost. Decision variables are the optimal power output requested from a TCL-aggregator (P_{TCL}^C), DGs' set-points (P_{G0}), ESSs' charge/discharge power (P_{ch}, P_{dch}), and RPCs set-points (Q_{comp}). The optimal power output (P_{TCL}^C) decided by the EMS and requested from a TCL-aggregator depends on the maximum available power for control (P_{max}^+, P_{max}^-) and is then used by the

aggregator for selecting TCLs that are due to participate in the secondary control. Accordingly, the TCLs receive the number of ON and OFF groups (N_{on} and N_{off}, respectively), group indicators (G_{ind}), as well as activation signals for up or down control (AC^+ and AC^-, respectively).

5.2 Power Flow based-Multi-Objective Optimization

5.2.1 Objective Functions

The PF based multi-objective optimization determines the optimal dispatch of the available regulating resources in order to simultaneously minimize one or more objective functions while considering power flow equations and constraints, as well as grid components' models and capacities. The available resources can be TCL-aggregators, dispatchable DGs, RPCs, ESSs, etc.

In general, for the case of a microgrid, the competitive objective functions to be minimized are frequency deviation, voltage deviation, and microgrid operation cost, defined as follows:

$$F_{\Delta f} = (f - f_0)^2 = (\Delta f)^2 \tag{5.1}$$

$$F_{\Delta V} = \sum_{i=1}^{U} (V - V_0)^2 \tag{5.2}$$

$$F_{Cost} = \sum C_i(P_{G,i}) \tag{5.3}$$

where $C_i(P_{G,i})$ is the generation cost of the DER i, U is the number of buses violating the permissible range. $F_{\Delta f}$ and $F_{\Delta V}$ are referred to as frequency deviation index (FDI) and voltage deviation index (VDI), respectively. The secondary control is achieved by the simultaneous minimization of objective functions (5.1), (5.2) and (5.3).

The resulting multi-objective optimization problem can be solved by a wide variety of optimization techniques. A simple but powerful method is the multi-objective particle swarm optimization (MOPSO). This technique is gaining increasing popularity in power system applications as it is an easy-to-implement, computationally efficient, and fast-convergent heuristic technique [94].

5.2.2 Active And Reactive Power Balance Equations

Three unknown variables namely voltage magnitude, angle and frequency are to be determined by the PF procedure. Compared with the conventional power flow procedure in which

only voltages and angles are state variables, the frequency is added as an additional state variable (unknown). Thus, the value of frequency can be determined after large deviations (e.g. contingency events) or in the case of an islanded operation of a microgrid [95]. The PF equations are constituted in a way that the mismatch between the calculated and specified active and reactive power injections at each bus is set to zero. It is noted that in this work, the power system is supposed to be balanced and the power flow is applied to the single-phase system. The active and reactive power mismatches at each bus i can be expressed in the form of non-linear equations as follows:

$$\Delta P_i = P_{Gi} + PV_i + PW_i + \sum_{j=1}^{N_i} (P_{dch,j} - P_{ch,j}) - P_{TLi} - \sum_{j=1}^{N_{bus}} V_i V_j Y_{ij} \cos(\delta_i - \delta_j - \theta_{ij})$$
(5.4)

$$\Delta Q_i = Q_{Gi} - Q_{TLi} - Q_{comp} - \sum_{j=1}^{N_{bus}} V_i V_j Y_{ij} \sin(\delta_i - \delta_j - \theta_{ij}) \tag{5.5}$$

where N_{bus} is the number of buses and N_i is the number of ESS units connected to bus i. P_{Gi} and Q_{Gi} are the injected active and reactive power of the DG at bus i. P_{dch} and P_{ch} are the ESS discharging and charging power, respectively. PV_i is the non-dispatchable photovoltaic power output, and PW_i is the non-dispatchable wind power output. P_{TLi} and Q_{TLi} are the total active and reactive load demands at bus i, and Q_{comp} is the compensated reactive power. V_i and δ_i denote the magnitude and angle of voltage at bus i, respectively. θ_{ij} and Y_{ij} are the magnitude and angle of the $(i,j)^{th}$ component of the system admittance-matrix, respectively.

5.2.3   Grid Components Modeling

Load Model

The total active and reactive load demands at each bus can be expressed as follows:

$$P_{TLi} = P_{TCL}^{NC} + P_{TCL,i}^{C}(P_{max,i}) + P_{Li} \tag{5.6}$$

$$Q_{TLi} = Q_{TCL,i}^{NC} + Q_{TCL,i}^{C}(Q_{max,i}) + Q_{Li} \tag{5.7}$$

where subscript i denotes the bus number. P_{TCL}^{C} and Q_{TCL}^{C} are the controllable active and reactive power components of the TCL population connected to bus i, respectively. These components represent the power output requested from a TCL-aggregator with a maximum active power of P_{max} and a maximum reactive power of Q_{max}, which are estimated using the neural network based aggregated model. The non-controllable active and reactive power components of the TCL-population are denoted by P_{TCL}^{NC} and Q_{TCL}^{NC}, respectively, and represent the aggregated power of the non-feasible bounds. The non-controllable power component of TCLs can be obtained from the neural network output by subtracting the

available power P_{max} from the aggregated power P_{agg}. P_{Li} and Q_{Li} are respectively the active and reactive powers associated to non-TCL loads as well as TCL loads which do not participate in the regulation. These powers can be represented by a polynomial static load model that accounts for voltage and frequency dependency [96]. The active and reactive power of a polynomial load at bus i is expressed as follows:

$$P_{Li} = P_{Loi}\left(1 + k_P^i\Delta f\right)\left(a_0^i + a_1^i\left(\frac{V_i}{V_0}\right) + a_2^i\left(\frac{V_i}{V_0}\right)^2\right) \tag{5.8}$$

$$Q_{Li} = Q_{Loi}\left(1 + k_Q^i\Delta f\right)\left(b_0^i + b_1^i\left(\frac{V_i}{V_0}\right) + b_2^i\left(\frac{V_i}{V_0}\right)^2\right) \tag{5.9}$$

where P_{Loi} and Q_{Loi} are respectively the nominal active and reactive power consumption. k_P^i and k_Q^i are the frequency sensitivity parameters while a_0^i, a_1^i and a_2^i are voltage sensitivity parameters for active power and their sum must be equal to unity as they represent the fraction of each load type in the bus. The same applies to b_0^i, b_1^i and b_2^i that are the voltage sensitivity parameters for the reactive power.

DG model

For a microgrid operating in grid-connected mode, generators are usually modeled as a conventional PV bus provided that its maximum and minimum reactive power thresholds are not violated. Otherwise, the generator becomes a PQ bus for which the reactive power is set to its maximum limit. Nevertheless, in case of islanded operation, the output power of each DG is adjusted with respect to its droop curve. Two types of dispatchable DGs are considered in this work: Synchronous-generator DGs (SG-DGs) and electronically-interfaced DGs (EI-DGs) [22].

SG-DG model: The active output power of an SG-DG is adjusted according to the following equations:

$$P_{Gi} = P_{Goi} - \frac{P_{Gi\_\max}}{R_i}(f - f_0) \tag{5.10}$$

$$P_{Gi\_\min} \leq P_{Gi} \leq P_{Gi\_\max} \tag{5.11}$$

where P_{Gi} and P_{Goi} are respectively the injected and set-point active power of the DG at bus i. R_i is the droop speed and subscripts max and min denote maximum and minimum values. As for the reactive power adjustment, many cases can be distinguished as reported in [97]. In this work, we consider two types; The first type is the SG-DG with Automatic Q regulator (AQR) that allows an operation of the DG with a constant power factor. In this

case, the active power is specified based on equations (5.10)-(5.11) while reactive power is regulated based on the following equations:

$$Q_{Gi} = Q_{Goi} - a_{Qi}\frac{P_{Gi\_max}}{R_i}(\Delta f) + b_{Qi}\left(\frac{P_{Gi\_max}}{R_i}(\Delta f)\right)^2 \tag{5.12}$$

$$Q_{Gi\_min} \leq Q_{Gi} \leq Q_{Gi\_max} \tag{5.13}$$

where Q_{Gi} and Q_{Goi} are respectively the injected and set-point active power. a_{Qi} and b_{Qi} represent reactive power generation coefficients.

The second type is the SG-DG with an automatic voltage regulator that allows an operation under constant voltage, only when the equation (5.13) is satisfied. Otherwise, the bus is converted to a PQ bus for which the reactive power is set to its maximum limit [22].

EI-DG model: This type of DG operates based on its droop curve that is governed by the following equations [22]:

$$P_{Gi} = P_{Goi} - \frac{P_{Gi\_max}}{m_i}(f - f_o) \tag{5.14}$$

$$Q_{Gi} = Q_{Goi} - \frac{Q_{Gi\_max}}{n_i}(V_i - V_{oi}) \tag{5.15}$$

where m_i and n_i are the active and reactive droop coefficients of the DG connected to the ith bus.

5.2.4 Trust Region-Based PF Solution

Power flow equations (5.4)-(5.5) result in a set of non-linear equations that can be cast in the following matrix form minimization problem:

$$F(X) = \begin{bmatrix} \Delta P \\ \Delta Q \end{bmatrix}^k \text{ where } X = \begin{bmatrix} \Delta(\Delta f) \\ \Delta \delta \\ \Delta V \end{bmatrix}^k \tag{5.16}$$

where F is the power mismatch vector described by equations (5.4)-(5.5).

Conventionally, this system is solved using the Newton-Raphson method based on the calculation of the Jacobian matrix and its inverse at each iteration. Although characterized by its fast convergence, this method faces convergence issues when dealing with distribution networks in general, and islanded microgrid in particular for several reasons. Islanded microgrids are prone to large disturbances and fall under the category of ill-conditioned systems

characterized by a narrow region of attraction. In this case, a flat initial guess can be far from the solution causing the Newton-Raphson method divergence [98]. Furthermore, an islanded microgrid is composed of small DGs of comparable sizes. Consequently, the power flow is formulated without a slack bus that has been always employed as mathematical artifact to tackle power flow infeasibility issues. Thus, absence of a slack bus results in a system operating close to infeasibility boundary [99, 100].

A robust equation-solving technique such as the Trust-region is therefore needed to reliably solve the PF equations and overcome all of the above-mentioned issues. The Trust-region constitutes a globally-convergent method for solving a non-linear system of equations. Moreover, the trust-region method is highly robust as it can manage cases of a singular Jacobian and an initial guess far from the solution. The Matlab function "fsolve" is a convenient tool for solving this problem and consequently obtaining the power flow solution. In particular, "trust-region-dogleg" can be used as a simple, efficient and robust strategy [101].

5.3   Case Study

To evaluate the effectiveness of the proposed control framework, a 21-bus islanded microgrid with a voltage level of 20kV and a power base of 10 MVA [22] is considered as shown in Figure 5.2. It is noted that in this work, the power system is supposed to be balanced and the power flow is applied to the single-phase system. The system comprises two SG-DGs at buses 9 and 21, three dispatchable EI-DGs at buses 13, 15 and 17. DGs in buses 13 and 15 are equipped with ESSs each with a capacity equal to 30% of the maximum power of their corresponding DG . Initially, ESSs are discharged up to 20 % of their maximum power. A PV unit at bus 19 is the only non-dispatchable generation unit and is assumed to have an initial power of 0.5280 MW. The coefficients for modeling DG units are taken from [22] and their characteristics inclusing the marginal cost of generation are illustrated in Table 5.1. The cost of DR provision is assumed to be 15 $/MWh [102].

Table 5.1 DGs characteristics [22].

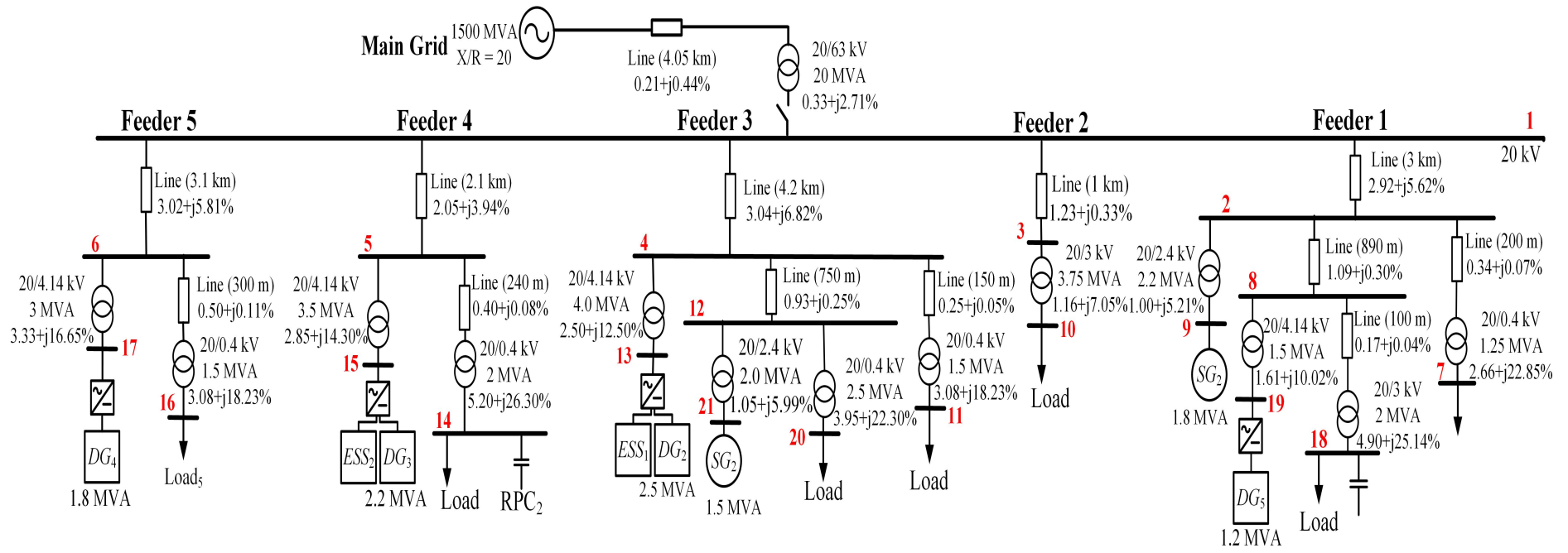| Bus	Type	P_{Gmin} (MW)	P_{max} (MW)	Q_{min} (MVar)	Q_{max} (MVar)	Inertia (p.u. sec)	Cost ($/MWh)
9	SG-DG, AVR	0	1.440	0	1.08	1.1881	65.6
13	EI-DG	-0.6	2	-1.5	1.5	-	43.2
15	EI-DG	-0.528	1.76	-1.32	1.32	-	39.1
17	EI-DG	-0.432	1.44	-1.08	1.08	-	27.7
21	SG-DG, AQR	0	1.2	0	0.9	1.6637	61.3

Figure 5.2 The studied 21-bus microgrid, adapted from [22].

The voltage and frequency dependent loads are connected to various buses. It is assumed that a certain portion of the load of each bus is dedicated to the TCL loads. Without loss of generality, a power factor of 0.85 is assumed at each load bus. Two RPCs are located at buses 14 and 18 with a capacity to increase the load power factor up to 0.95. Initially DGs are operating at their maximum power output. We suppose that the test microgrid undergoes a severe deviation that should be corrected by the proposed EMS through participation of TCL aggregators. It is assumed that an acceptable VDI should be below 0.025 and the reference frequency is 50Hz.

5.3.1 Comparision of the Newton-Raphson and Trust-region methods

In this part, the convergence of the developed Trust region-based PF method is tested and compared with the Newton-Raphson method. The classical MATPOWER package have been edited to implement the Trust region-based PF. It is known that the power flow method
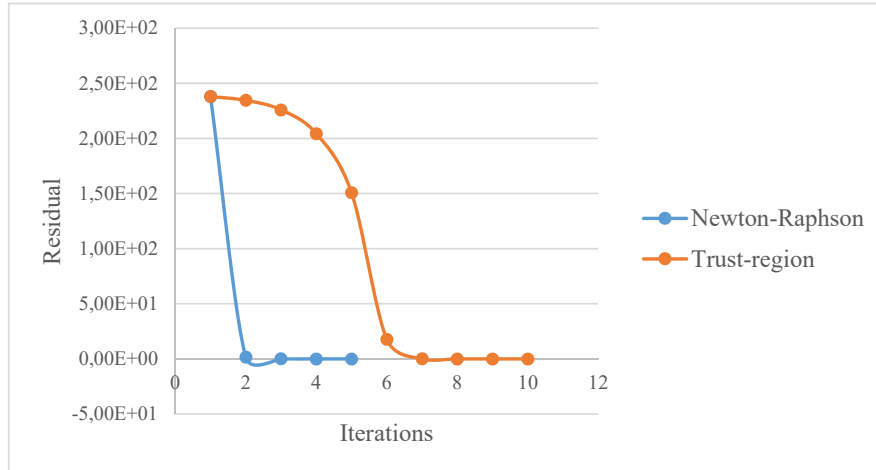
Figure 5.3 Case 1: Comparision of the convergence of the Newton-Raphson and the Trust-region methods.

converges when the norm of the power mismatch vector also called the residual is less than a predefined tolerance ϵ. The tolerance is set to 10^{-5}. Two cases are considered; In the first case, slight load deviations are randomly generated at different buses in order to have initial guesses slightly far from the solution. It is noted that the initial guess of the voltage, angle, and frequency are 1 p.u., 0°, and 50Hz. In the second case, a large deviation at bus 16 is

simulated by multiplying the initial power by 10. Figure 5.3 and Figure 5.4 show the residuals versus the iterations for cases 1 and 2, respectively. In the first case, both methods converge,
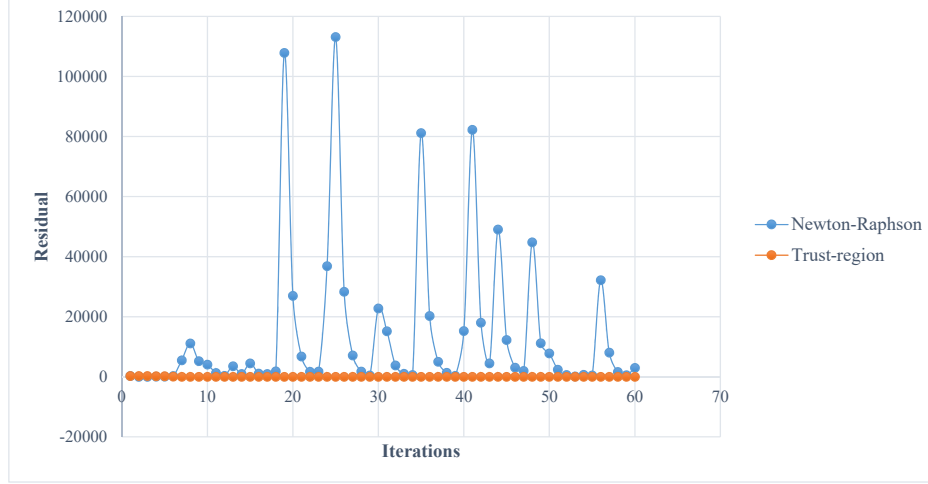
Figure 5.4 Case 2: Comparision of the convergence of the Newton-Raphson and the Trust-region methods.

however, the convergence of the Newton-Raphson method occurs faster and with only a few iterations (see Figure 5.3). This case can be classified as 'safe' as the initial guess is not so far from the solution [103]. The extreme deviation in the second case causes the divergence of the Newton-Raphson method, as shown in Figure 5.4. The residuals of the Newton-Raphson method largely fluctuate even after a large number of iterations. In contrast, the Trust-region method has stable behavior.

It can be concluded, that in the cases in which the initial guess is close to the solution, both methods converge while the Newton-Raphson outperforms the Trust-region method in terms of the speed of convergence. In the case of large deviations as in case of contingencies, the Trust-region method slowly converges while the Newton-Raphson method diverges with a highly volatile behavior [103].

5.3.2   Case of a Large deviation

We consider the case of a severe frequency deviation caused by 10% of load increase following which the TCL aggregations at buses 14 and 16 participate in the primary control, each modeled by its equivalent droop characteristic with a primary control reserve equal to 0.45

MW. As the deviation is large, all the primary control reserve is released resulting in a steady-state frequency of 49.9037 Hz and a VDI equal to 0.0268 as shown in Table 5.2 which report violation from pre-specified permissible limits while DGs operate at their maximum output. Voltage profile at different buses is shown in Figure 5.5 confirming a severe under-voltage at all microgrid buses. To apply the secondary control, the trained neural network is used to estimate the amount of the secondary control reserve at buses 7, 10, 11 and 20 that consist of 150, 400, 250 and 300 TCLs, respectively based on voltage and frequency obtained from the PF.

Table 5.2 Simulation results of different scenarios for secondary regulation (BC: before control, AC: after control).

		BC			AC								
Scenario		Intial			Scenario 1: Only TCLs					Scenario 2: TCL+RPC+ESSs			
Frequency		49.9037			49.9961					49.9927			
VDI		0.0268			0.0079					0.0000			
Total Cost ($)		360.0488			317.9323					273.6657			
Bus		P_{TL}/P_{G0}	Q_{L0}/Q_{G0}	Q_{comp}	P_{TL}/P_{G0}	Q_{TL}/Q_{G0}	Q_{comp}	P_{TCL}	Q_{TCL}	P_{TL}/P_{G0}	Q_{TL}/Q_{G0}	P_{dch}	Q_{comp}
Load	7	0.9500	0.5268	-	0.7538	0.4671	-	0.2045	0.1267	0.7525	0.4664	-	-
	10	2.500	1.4437	-	2.1819	1.3498	-	0.3587	0.2223	1.9007	1.1768	-	-
	11	0.8500	0.5280	-	0.5973	0.3702	-	0.2596	0.1609	0.4389	0.2720	-	-
	14	0.700	0.6912	0.0905	0.6957	0.4305	0.0905	-	-	0.6974	0.4318	-	0.1778
	16	0.8800	0.4834	-	0.8800	0.5454	-	-	-	0.8800	0.5454	-	0.2226
	18	0.8500	0.7792	0.0075	0.8433	0.5217	0.0075	-	-	0.8466	0.5243	-	-
	20	1.7600	0.8183	-	1.5552	0.9617	-	0.2532	0.1569	1.3416	0.8304	-	-
Generation	9	1.1400	-	-	1.1400	.0.0000	-	-	-	1.1400	0.0000	-	-
	13	2.0120	1.2676	-	2.0120	1.2676	-	-	-	2.0120	1.2676	0.6620	-
	15	1.4656	1.0361	-	1.4656	1.0361	-	-	-	1.4656	1.0361	0.3224	-
	17	1.2264	0.9825	-	1.2264	0.9825	-	-	-	1.2264	0.9825	-	-
	19	1	0.0000	-	0.5280	0.0000	-	-	-	0.5280	0.0000	-	-
	21	1.1648	0.8182	-	1.1648	0.8182	-	-	-	1.1648	0.8182	-	-

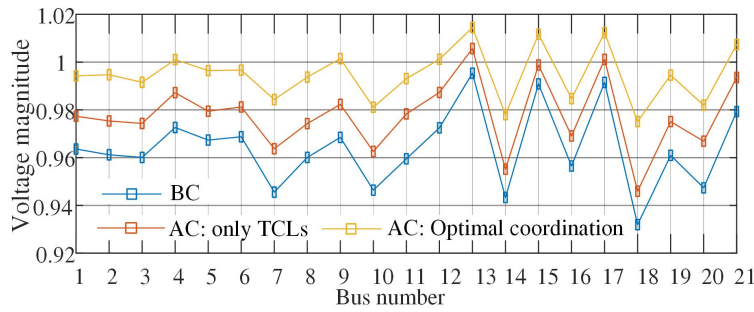Figure 5.5 Voltage magnitude at different buses before and after control considering different scenarios (BC: before control, AC: after control).

Two scenarios are considered; In the first one, FDI and VDI are corrected by the TCLs only. In the second one, an optimal coordination among TCLs, RPCs and ESSs is adopted and the new optimal amount of active and/or reactive power to be injected by loads and RPCs are

calculated. The optimal coordination yields also the amount of the discharge power of the ESSs. Simulation results are illustrated in Table 5.2 that shows the new optimal set-points for the involved resources as well as the resulting FDI and VDI. The voltage profile at microgrid buses are shown in Figure 5.5. It is seen that TCLs succeed in restoring the FDI and the VDI to their permissible dead-band. This is owing to the fact that TCLs are distributed on different buses and have the capability to change both active and reactive power injections to the bus. However, the cost is only reduced by 11.7%. These results are further improved in case of an optimal coordination as the VDI is minimized to zero and the frequency is restored to the dead-band zone while the cost is reduced by 24% as the ESS share the imbalance with no cost. These results confirm the effectiveness of the proposed method for the primary and secondary control and suggest optimal coordination among TCLs and other grid resources for obtaining an improved performance.

From the results presented in this Section, it is found that the proposed method succeeds to correct both VDI and FDI while reducing the operation cost of the microgrid.

5.4 Conclusion

In this chapter, a hierarchical control based EMS for primary and secondary frequency and voltage control of a microrid has been proposed. In this framework, aggregations of TCLs participate in the control task together with other grid ressources, and the participation of TCLs is managed by a TCL aggregator. As the provision of primary frequency control has been tackled in Chapter 4, this Chapter has mainly focused on the provision of the secondary control. To this aim, the secondary contorl is formulated as a multi-objective optimization problem with the objective of simultaneously minimizing the voltage/frequency deviations and grid operation cost. To overcome the convergence issues of the clasical Newton-Raphson method, the Trust-region method has been used to reliably solve the PF equations. A 21-bus islanded microgrid has been considered. It has been shown that TCLs succeed in suppressing frequency and voltage deviations, however lower grid operation cost can be obtained when aggregations of TCLs cooperate with other grid ressources such as the ESSs.

CHAPTER 6   CONCLUSION AND FUTURE WORK

DR is considered as a promising and alluring option for responding to the increasing need of control reserves. In particular, TCLs are considered as a potential candidate mainly due to their fast-acting feature, wide distribution in the grid, and their ability to participate in control services without compromising the end-user comfort. However, for a realistic implication of TCLs in control reserve provision, various challenges should be addressed. First, as a single TCL has a negligible contribution to the demand side, it is essential to aggregate large numbers of TCLs to be able to participate in the provision of control reserves. To this aim, the development of an accurate yet straightforward aggregated model is needed to estimate and predict the available flexibility offered by TCLs. A neural network based approach has been therefore developed to this aim and compared with the classical Markov Chain approach. Results presented in this report showed that the proposed approach outperforms the classical Markov Chain approach in terms of prediction accuracy even for relatively longer prediction horizons. Moreover, the neural network approach allows to accurately take into account the effect of ambient temperature, the voltage, and the frequency on the dynamic behaviour of a TCL population.

It has also been discussed in this report that to develop fast-reacting and reliable control hierarchy the customer comfort should be always maintained which is rather challenging. In particular, the TCL temperature must remain within its predefined dead-band, the number of switching events should be minimized, and the short-cycling should be reduced. To this aim, based on the available control reserves, control methods that allow the management of TCL populations as virtual generators for primary and secondary control have been developed. An aggregator is needed as an intermediate unit to manage the participation of TCLs in the ancillary services market. The aggregator sends control signals to the TCLs in order to obtain a collective response that emulates the behavior of conventional generators. TCLs have been divided into groups that take turns in responding to deviations or control signals coming from the aggregator. Moreover, it has been discussed that a proper prioritization of TCLs based on their temperature allows minimizing the number of switching events. To meet the requirements of primary frequency control, TCLs participation in primary frequency control has been selected to be semi-autonomous which implies that TCLs' response to local deviations is instantaneous while they regularly receive control parameters from the aggregator at relatively long control intervals. Simulation results showed that a proper definition of the control parameters allows obtaining a collective response of a TCL population similar to the droop-based behavior of conventional generators with the communication burden

significantly reduced. Simulation results also showed that the TCL participation in primary control reduces frequency fluctuations. Furthermore, when coordinated with conventional generators, the proposed control method results in an improved dynamic and steady-state frequency response. As the secondary control is less demanding than the primary control in terms of response speed, it is performed in a centralized way as TCLs receive direct ON/OFF switching signals from an aggregator. In this case, the control method allows changing the aggregated power consumption of TCLs is similar to the the way that the output power of conventional generators is changed.

Finally, a hierarchical control based EMS has been proposed to enable aggregations of TCLs to participate in the primary and secondary control of a microgrid, in coordination with the conventional grid resources. In particular, the secondary control has been formulated as a PF-based multi-objective optimization in order to minimize frequency and voltage deviations as well as grid operation cost. The trust-region method is adopted to reliably solve PF equations, and the multi-objective particle swarm optimization has been used to solve the optimization problem. Only TCLs that have active and reactive power consumption were allowed to participate in the secondary control so that they could affect both active and reactive power flows. The simulated case studies showed that TCLs' participation in the provision of control reserves allows the suppression of frequency and voltage deviation while reducing the grid operation cost. Improved performance has been obtained when TCLs participate in the control task in coordination with conventional grid resources such as the ESSs.

This work can be further extended in three directions. First, similar to the management of TCL populations for the provision of control reserves, appropriate control methods can be developed for the management of electric vehicles as virtual generators. In this way, it is of great interest to investigate the optimal coordination between populations of TCLs and electric vehicles for the provision of control reserves.

Furthermore, as the reservation of control reserves is considered out of the scope of this work, a day-ahead scheduling process can be developed to optimally allocate the operation mode of each TCL with a one-hour time window. In addition to the PCM and SCM, TCLs can have other modes such as peak shaving mode. From one hand, this day-ahead scheduling allows organizing the participation of different grid resources along with TCL aggregators. This helps to avoid conflicts and to reach an agreement among different resources in terms of regulation services provision. From the other hand, such scheduling allows leveraging the full potential of TCLs as it as it extends their participation in various ancillary services.

Finally, one may be interested to consider the uncertainties of the TCLs and the renewable

generation in modeling and aggregation procedure by making use of more rigorous control approaches such as robust control.

REFERENCES

[1] Drax Group. (2018) The great balancing act: what it takes to keep the power grid stable. [Online]. Available: https://www.drax.com/technology/great-balancing-act-takes-keep-power-grid-stable/

[2] M. D. Ilić and S. Liu, *Structural Modeling and Control Design Using Interaction Variables.* London: Springer London, 1996, pp. 61–81. [Online]. Available: https://doi.org/10.1007/978-1-4471-3461-9_4

[3] Y. G. Rebours *et al.*, "A survey of frequency and voltage control ancillary services—part i: Technical features," *IEEE Transactions on power systems*, vol. 22, no. 1, pp. 350–357, 2007.

[4] A. Bidram and A. Davoudi, "Hierarchical structure of microgrids control system," *IEEE Transactions on Smart Grid*, vol. 3, no. 4, pp. 1963–1976, 2012.

[5] CBC. (2016) Justin trudeau signs paris climate treaty at un, vows to harness renewable energy. [Online]. Available: https://www.cbc.ca/news/politics/paris-agreement-trudeau-sign-1.3547822

[6] Prairie Climate Centre. (2018) How does canada plan to reduce its greenhouse gas footprint? [Online]. Available: http://prairieclimatecentre.ca/2018/05/how-does-canada-plan-to-reduce-its-greenhouse-gas-footprint/

[7] Energy policies of iea countries: Denmark 2011 review. [Online]. Available: http://bit.ly/1RBf6Vs

[8] Z. A. Obaid *et al.*, "Frequency control of future power systems: reviewing and evaluating challenges and new control methods," *Journal of Modern Power Systems and Clean Energy*, vol. 7, no. 1, pp. 9–25, 2019.

[9] N. Lu, P. Du, and Y. V. Makarov, "The potential of thermostatically controlled appliances for intra-hour energy storage applications," in *2012 IEEE Power and Energy Society General Meeting.* IEEE, 2012, pp. 1–6.

[10] Q. Hu *et al.*, "An approach to assess the responsive residential demand to financial incentives," in *2015 Ieee power & energy society general meeting.* IEEE, 2015, pp. 1–5.

[11] A. Losi, P. Mancarella, and A. Vicino, *Demand Response in Smart Grids.* John Wiley & Sons, Ltd, 2015, ch. 1, pp. 1–10. [Online]. Available: https://onlinelibrary.wiley.com/doi/abs/10.1002/9781119245636.ch1

[12] H. Yang *et al.*, "Demand response of inverter air conditioners and applications in distribution system voltage stability enhancement," in *2013 International Conference on Electrical Machines and Systems (ICEMS)*, Oct 2013, pp. 954–959.

[13] Natural Resources Canada. (2019) Heating equipment for residential use. [Online]. Available: https://www.nrcan.gc.ca/energy/products/categories/heating/13740

[14] International Energy Agency. (2018) Air conditioning use emerges as one of the key drivers of global electricity-demand growth. [Online]. Available: https://www.iea.org/newsroom/news/2018/may/air-conditioning-use-emerges-as-one-of-the-key-drivers-of-global-electricity-dema.html

[15] B. J. Kirby, *Demand Response For Power System Reliability: FAQ.* Citeseer, 2006.

[16] S. Acharya *et al.*, "A control strategy for voltage unbalance mitigation in an islanded microgrid considering demand side management capability," *IEEE Transactions on Smart Grid*, 2018.

[17] B. J. Kirby, *Spinning reserve from responsive loads.* Citeseer, 2003.

[18] D. S. Callaway and I. A. Hiskens, "Achieving controllability of electric loads," *Proceedings of the IEEE*, vol. 99, no. 1, pp. 184–199, 2010.

[19] V. Trovato *et al.*, "Advanced control of thermostatic loads for rapid frequency response in great britain," *IEEE Transactions on Power Systems*, vol. 32, no. 3, pp. 2106–2117, 2016.

[20] E. Vrettos and G. Andersson, "Combined load frequency control and active distribution network management with thermostatically controlled loads," in *2013 IEEE International Conference on Smart Grid Communications (SmartGridComm)*. IEEE, 2013, pp. 247–252.

[21] S. C. Ross, G. Vuylsteke, and J. L. Mathieu, "Effects of load-based frequency regulation on distribution network operation," *IEEE Transactions on Power Systems*, vol. 34, no. 2, pp. 1569–1578, 2018.

[22] M. Bayat *et al.*, "Coordination of distributed energy resources and demand response for voltage and frequency support of mv microgrids," *IEEE Transactions on Power Systems*, vol. 31, no. 2, pp. 1506–1516, 2016.

[23] P. Cappers, C. Goldman, and D. Kathan, "Demand response in us electricity markets: Empirical evidence," *Energy*, vol. 35, no. 4, pp. 1526–1535, 2010.

[24] Y.-K. Wu and K.-T. Tang, "Frequency support by demand response–review and analysis," *Energy Procedia*, vol. 156, pp. 327–331, 2019.

[25] M. H. Albadi and E. F. El-Saadany, "A summary of demand response in electricity markets," *Electric power systems research*, vol. 78, no. 11, pp. 1989–1996, 2008.

[26] "Benefits of demand response in electricity markets and recommendations for achieving them," U.S. Department of Energy, Rapport technique, 2006.

[27] M. H. Albadi and E. F. El-Saadany, "Demand response in electricity markets: An overview," in *2007 IEEE power engineering society general meeting.* IEEE, 2007, pp. 1–5.

[28] M. Lee *et al.*, "Assessment of demand response and advanced metering," *Federal Energy Regulatory Commission, Tech. Rep*, 2013.

[29] O. G. Ibe and A. I. Onyema, "Concepts of reactive power control and voltage stability methods in power system network," *IOSR Journal of Computer Engineering*, vol. 11, no. 2, pp. 15–25, 2013.

[30] J. Seymour and T. Horsley, "The seven types of power problems," *APC, USA*, 2005.

[31] H. Haes Alhelou *et al.*, "A survey on power system blackout and cascading events: Research motivations and challenges," *Energies*, vol. 12, no. 4, p. 682, 2019.

[32] A. LA BELLA, "Predictive control of voltages and frequency in an islanded microgrid," 2015.

[33] H. Laaksonen, P. Saari, and R. Komulainen, "Voltage and frequency control of inverter based weak lv network microgrid," in *2005 International Conference on Future Power Systems*, Nov 2005, pp. 6 pp.–6.

[34] P. Kundur, N. J. Balu, and M. G. Lauby, *Power system stability and control.* McGraw-hill New York, 1994, vol. 7.

[35] R. D'hulst *et al.*, "Voltage and frequency control for future power systems: the electra irp proposal," in *2015 International Symposium on Smart Electric Distribution Systems and Technologies (EDST)*. IEEE, 2015, pp. 245–250.

[36] G. Lou *et al.*, "Distributed mpc-based secondary voltage control scheme for autonomous droop-controlled microgrids," *IEEE Transactions on Sustainable Energy*, vol. 8, no. 2, pp. 792–804, April 2017.

[37] Y. Rebours, "A comprehensive assessment of markets for frequency and voltage control ancillary services," Ph.D. dissertation, university of Manchester, 2008.

[38] V. Trovato, F. Teng, and G. Strbac, "Role and benefits of flexible thermostatically controlled loads in future low-carbon systems," *IEEE Transactions on Smart Grid*, vol. 9, no. 5, pp. 5067–5079, Sep. 2018.

[39] S. Izadkhast, P. Garcia-Gonzalez, and P. Frías, "An aggregate model of plug-in electric vehicles for primary frequency control," *IEEE Transactions on Power Systems*, vol. 30, no. 3, pp. 1475–1482, 2014.

[40] S. Vandael *et al.*, "A comparison of two giv mechanisms for providing ancillary services at the university of delaware," in *2013 IEEE international conference on smart grid communications (SmartGridComm)*. IEEE, 2013, pp. 211–216.

[41] S. Izadkhast *et al.*, "An aggregate model of plug-in electric vehicles including distribution network characteristics for primary frequency control," *IEEE Transactions on Power Systems*, vol. 31, no. 4, pp. 2987–2998, 2015.

[42] H. Hao *et al.*, "Aggregate flexibility of thermostatically controlled loads," *IEEE Transactions on Power Systems*, vol. 30, no. 1, pp. 189–198, 2014.

[43] W. Wenting *et al.*, "Hierarchical and distributed demand response control strategy for thermostatically controlled appliances in smart grid," *Journal of Modern Power Systems and Clean Energy*, vol. 5, no. 1, pp. 30–42, 2017.

[44] R. Malhame and C.-Y. Chong, "Electric load model synthesis by diffusion approximation of a high-order hybrid-state stochastic system," *IEEE Transactions on Automatic Control*, vol. 30, no. 9, pp. 854–860, 1985.

[45] N. Lu, D. P. Chassin, and S. E. Widergren, "Modeling uncertainties in aggregated thermostatically controlled loads using a state queueing model," *IEEE Transactions on Power Systems*, vol. 20, no. 2, pp. 725–733, 2005.

[46] D. S. Callaway, "Tapping the energy storage potential in electric loads to deliver load following and regulation, with application to wind energy," *Energy Conversion and Management*, vol. 50, no. 5, pp. 1389–1400, 2009.

[47] J. L. Mathieu, S. Koch, and D. S. Callaway, "State estimation and control of electric loads to manage real-time energy imbalance," *IEEE Transactions on power systems*, vol. 28, no. 1, pp. 430–440, 2012.

[48] J. L. Mathieu *et al.*, "Energy arbitrage with thermostatically controlled loads," in *2013 European Control Conference (ECC).* IEEE, 2013, pp. 2519–2526.

[49] S. Koch, J. L. Mathieu, and D. S. Callaway, "Modeling and control of aggregated heterogeneous thermostatically controlled loads for ancillary services," in *Proc. PSCC.* Citeseer, 2011, pp. 1–7.

[50] J. L. Mathieu and D. S. Callaway, "State estimation and control of heterogeneous thermostatically controlled loads for load following," in *2012 45th Hawaii International Conference on System Sciences.* IEEE, 2012, pp. 2002–2011.

[51] W. Zhang *et al.*, "Aggregated modeling and control of air conditioning loads for demand response," *IEEE Transactions on power systems*, vol. 28, no. 4, pp. 4655–4664, 2013.

[52] Y.-J. Kim, L. K. Norford, and J. L. Kirtley, "Modeling and analysis of a variable speed heat pump for frequency regulation through direct load control," *IEEE Transactions on Power Systems*, vol. 30, no. 1, pp. 397–408, 2014.

[53] S. Koch, M. Zima, and G. Andersson, "Active coordination of thermal household appliances for load management purposes," *IFAC Proceedings Volumes*, vol. 42, no. 9, pp. 149–154, 2009.

[54] N. Lu, "An evaluation of the hvac load potential for providing load balancing service," *IEEE Transactions on Smart Grid*, vol. 3, no. 3, pp. 1263–1270, 2012.

[55] N. A. Daher *et al.*, "Improved control method of hvac system for demand response," in *2018 4th International Conference on Renewable Energies for Developing Countries (REDEC).* IEEE, 2018, pp. 1–6.

[56] P. Zhao *et al.*, "Dynamic frequency regulation resources of commercial buildings through combined building system resources using a supervisory control methodology," *Energy and buildings*, vol. 86, pp. 137–150, 2015.

[57] S. Weckx, R. D'hulst, and J. Driesen, "Primary and secondary frequency support by a multi-agent demand control system," *IEEE Transactions on Power Systems*, vol. 30, no. 3, pp. 1394–1404, 2014.

[58] Z. Xu, J. Ostergaard, and M. Togeby, "Demand as frequency controlled reserve," *IEEE Transactions on power systems*, vol. 26, no. 3, pp. 1062–1071, 2010.

[59] X. Rui, X. Liu, and J. Meng, "Dynamic frequency regulation method based on thermostatically controlled appliances in the power system," *Energy Procedia*, vol. 88, pp. 382–388, 2016.

[60] J. A. Short, D. G. Infield, and L. L. Freris, "Stabilization of grid frequency through dynamic demand control," *IEEE Transactions on power systems*, vol. 22, no. 3, pp. 1284–1293, 2007.

[61] K. Samarakoon, J. Ekanayake, and N. Jenkins, "Investigation of domestic load control to provide primary frequency response using smart meters," *IEEE Transactions on Smart Grid*, vol. 3, no. 1, pp. 282–292, 2011.

[62] Y.-Q. Bao *et al.*, "Design of a hybrid hierarchical demand response control scheme for the frequency control," *IET Generation, Transmission & Distribution*, vol. 9, no. 15, pp. 2303–2310, 2015.

[63] Q. Shi *et al.*, "A hybrid dynamic demand control strategy for power system frequency regulation," *CSEE Journal of Power and Energy Systems*, vol. 3, no. 2, pp. 176–185, 2017.

[64] S. H. Tindemans, V. Trovato, and G. Strbac, "Decentralized control of thermostatic loads for flexible demand response," *IEEE Transactions on Control Systems Technology*, vol. 23, no. 5, pp. 1685–1700, 2015.

[65] H. Zhao *et al.*, "Hierarchical control of thermostatically controlled loads for primary frequency support," *IEEE Transactions on Smart Grid*, vol. 9, no. 4, pp. 2986–2998, 2016.

[66] X. Wu *et al.*, "Hierarchical control of residential hvac units for primary frequency regulation," *IEEE Transactions on Smart Grid*, vol. 9, no. 4, pp. 3844–3856, 2017.

[67] B. Biegel *et al.*, "Primary control by on/off demand-side devices," *IEEE Transactions on Smart Grid*, vol. 4, no. 4, pp. 2061–2071, 2013.

[68] V. Lakshmanan *et al.*, "Provision of secondary frequency control via demand response activation on thermostatically controlled loads: Solutions and experiences from denmark," *Applied Energy*, vol. 173, pp. 470–480, 2016.

[69] A. Bokhari *et al.*, "Experimental determination of the zip coefficients for modern residential, commercial, and industrial loads," *IEEE Transactions on Power Delivery*, vol. 29, no. 3, pp. 1372–1381, 2013.

[70] K. McKenna and A. Keane, "Open and closed-loop residential load models for assessment of conservation voltage reduction," *IEEE Transactions on Power Systems*, vol. 32, no. 4, pp. 2995–3005, 2016.

[71] R. Garcia-Valle *et al.*, "Smart demand for improving short-term voltage control on distribution networks," *IET generation, transmission & distribution*, vol. 3, no. 8, pp. 724–732, 2009.

[72] Z. Akhtar, B. Chaudhuri, and S. Y. R. Hui, "Primary frequency control contribution from smart loads using reactive compensation," *IEEE Transactions on Smart Grid*, vol. 6, no. 5, pp. 2356–2365, 2015.

[73] J. Yi *et al.*, "Distribution network voltage control using energy storage and demand side response," in *2012 3rd IEEE PES Innovative Smart Grid Technologies Europe (ISGT Europe)*.   IEEE, 2012, pp. 1–8.

[74] Y. He and M. Petit, "Valorization of demand response for voltage control in mv distribution grids with distributed generation," in *2016 IEEE International Energy Conference (ENERGYCON)*.   IEEE, 2016, pp. 1–6.

[75] A. Zakariazadeh *et al.*, "A new approach for real time voltage control using demand response in an automated distribution system," *Applied Energy*, vol. 117, pp. 157–166, 2014.

[76] K. Christakou *et al.*, "Gecn: Primary voltage control for active distribution networks via real-time demand-response," *IEEE Transactions on Smart Grid*, vol. 5, no. 2, pp. 622–631, 2013.

[77] M. Brenna *et al.*, "Voltage control in smart grids: An approach based on sensitivity theory," *Journal of Electromagnetic Analysis and Applications*, vol. 2, no. 08, p. 467, 2010.

[78] M. T. Hagan *et al.*, *Neural network design.*   Pws Pub. Boston, 1996, vol. 20.

[79] DIGITAL TRENDS. (2019) What is an artificial neural network? here's everything you need to know. [Online]. Available: https://www.digitaltrends.com/cool-tech/what-is-an-artificial-neural-network/

[80] G. Bebis and M. Georgiopoulos, "Feed-forward neural networks," *IEEE Potentials*, vol. 13, no. 4, pp. 27–31, Oct 1994.

[81] M. H. Beale, M. T. Hagan, and H. B. Demuth, "Neural network toolbox," *User's Guide, MathWorks*, vol. 2, pp. 77–81, 2010.

[82] R. E. Mortensen and K. P. Haggerty, "A stochastic computer model for heating and cooling loads," *IEEE Transactions on Power Systems*, vol. 3, no. 3, pp. 1213–1219, 1988.

[83] K. Lindén and I. Segerqvist, "Modelling of load devices and studying load/system characteristics," *Comput. Eng*, no. 131, p. 151, 1992.

[84] W. Price *et al.*, "Load representation for dynamic performance analysis," *IEEE Transactions on Power Systems (Institute of Electrical and Electronics Engineers);(United States)*, vol. 8, no. 2, 1993.

[85] IEEE Power & Energy Society. (2019) Open data sets. [Online]. Available: http://sites.ieee.org/pes-iss/data-sets/

[86] Voltage Disturbance Power Engineering Study Resource. Voltage tolerance standard – ansi c84.1. [Online]. Available: http://voltage-disturbance.com/voltage-quality/voltage-tolerance-standard-ansi-c84-1/

[87] P. Cramton, "Electricity market design," *Oxford Review of Economic Policy*, vol. 33, no. 4, pp. 589–612, 11 2017. [Online]. Available: https://doi.org/10.1093/oxrep/grx041

[88] Y. G. Rebours *et al.*, "A survey of frequency and voltage control ancillary services—part ii: Economic features," *IEEE Transactions on power systems*, vol. 22, no. 1, pp. 358–366, 2007.

[89] I. Würth *et al.*, "Minute-scale forecasting of wind power—results from the collaborative workshop of iea wind task 32 and 36," *Energies*, vol. 12, no. 4, p. 712, 2019.

[90] C. M. Grinstead and J. L. Snell, "Markov chains," *Introduction to probability*, pp. 405–470, 1997.

[91] B. Yu-Qing *et al.*, "Demand response for frequency control of multi-area power system," *Journal of Modern Power Systems and Clean Energy*, vol. 5, no. 1, pp. 20–29, 2017.

[92] E. Namor *et al.*, "Control of battery storage systems for the simultaneous provision of multiple services," *IEEE Transactions on Smart Grid*, 2018.

[93] H. Gerard, E. Rivero, and D. Six, "Basic schemes for tso-dso coordination and ancillary services provision," *SMARTNET Deliv. D*, vol. 1, 2016.

[94] M. R. AlRashidi and M. E. El-Hawary, "A survey of particle swarm optimization applications in electric power systems," *IEEE Transactions on Evolutionary Computation*, vol. 13, no. 4, pp. 913–918, 2008.

[95] M. Bayat, K. Sheshyekani, and A. Rezazadeh, "A unified framework for participation of responsive end-user devices in voltage and frequency control of the smart grid," *IEEE Transactions on Power Systems*, vol. 30, no. 3, pp. 1369–1379, 2014.

[96] W. Price *et al.*, "Load representation for dynamic performance analysis," *IEEE Transactions on Power Systems (Institute of Electrical and Electronics Engineers);(United States)*, vol. 8, no. 2, 1993.

[97] M. Okamura *et al.*, "A new power flow model and solution method including load and generator characteristics and effects of system control devices," *IEEE Transactions on Power Apparatus and Systems*, vol. 94, no. 3, pp. 1042–1050, 1975.

[98] M. M. A. Abdelaziz *et al.*, "A novel and generalized three-phase power flow algorithm for islanded microgrids using a newton trust region method," *IEEE Transactions on Power Systems*, vol. 28, no. 1, pp. 190–201, 2012.

[99] A. G. Expósito, J. L. M. Ramos, and J. R. Santos, "Slack bus selection to minimize the system power imbalance in load-flow studies," *IEEE Transactions on power systems*, vol. 19, no. 2, pp. 987–995, 2004.

[100] M. N. Madhu, N. Sasidharan, and J. G. Singh, "Droop control incorporated power flow method for distribution and microgrid systems," in *2015 IEEE Innovative Smart Grid Technologies-Asia (ISGT ASIA)*. IEEE, 2015, pp. 1–5.

[101] MathWorks. (2018) Equation solving algorithms. Visited on 2019-06-24. [Online]. Available: https://www.mathworks.com/help/optim/ug/equation-solving-algorithms.html

[102] M. Hummon, "Value of demand response: Quantities from production cost modeling (presentation)," National Renewable Energy Lab.(NREL), Golden, CO (United States), Tech. Rep., 2014.

[103] M. De Beurs *et al.*, "Optimal configuration of future electricity grid," *DIAM TU Delft Technical Report*, pp. 16–01, 2016.